공학박사학위논문

Simulation Study of the New Combustion Strategy of Pre-combustion-assisted Compression Ignition for Internal Combustion Engine Fueled by Pure Ammonia

예연소를 활용하는 암모니아 압축착화엔진 연소전략 개발 및 시뮬레이션 연구

2018 년 2 월

서울대학교 대학원

기계항공공학부

이 동 근

Abstract

Simulation Study of the New Combustion Strategy of Pre-combustion-assisted Compression Ignition for Internal Combustion Engine Fueled by Pure Ammonia

Donggeun Lee

Department of Mechanical Engineering

The Graduate School

Seoul National University

In recent years, with the increase in the spread of the renewable energy and the development of its technologies, the necessity of development of energy storage medium technology for storing renewable energy which is intermittent. Hydrogen is one of the energy storage media that has received much attention. There have been many studies on the use of hydrogen as fuel and energy storage in the form of hydrogen. However, since hydrogen has an

extremely low boiling point, it is difficult to store the hydrogen as a liquid phase, and when stored in a high-pressure gas phase, the energy density of the hydrogen based on volume is somewhat lowered. Ammonia is an energy storage medium that can compensate for the drawbacks of hydrogen. Since ammonia does not contain carbon in its molecular structure like hydrogen, it does not produce carbon-related emission during combustion, and has a merit of storability and transportability because it is in a liquid phase under a condition of room temperature and 10 atm.

Focusing on the possibility of using ammonia as a hydrogen carrier, a combustion strategy for pure ammonia as an engine fuel to convert the stored energy into a usable form has been proposed, which uses ammonia itself as a combustion promotor. Under this strategy, the conditions of sufficiently high temperature and pressure to cause the spray combustion of ammonia are obtained by the auto-ignition of a pilot-injected mixture of air and ammonia. To confirm the feasibility and the operating characteristics of an engine with the ammonia combustion strategy proposed in this study, engine modeling has been conducted, the combustion strategy has been simulated, and a parametric study has been performed. To analyze the mechanisms of NO production in an engine with the proposed combustion strategy, the NO production process has been classified into four phases, and the NO production in each phase has been analyzed under various start of injection timing and fuel amounts.

Keywords: Ammonia, Energy storage medium, Internal combustion engine, Combustion strategy, Engine modeling

***Identification Number*: 2011-20731**

Contents

List of Figures

List of Tables

Chapter 1. Introduction

1.1 Research background

With the gradual increase in the use of renewable energy as shown in Fig 1. 1 [1], the need for energy storage technology and the speed of research and development have rapidly increased. The energy storage technology is important since it enables the use of electricity to be efficient by utilizing the extra energy, which is stored during light duty period, in on-peak period.

Hydrogen is one of the most actively studied energy storage media. Focusing on the environment-friendly characteristics of hydrogen as a fuel, storage of hydrogen in form of high pressure gas and using metal hydrides have been studied [2-6]. In addition, much research has been conducted on the use of such stored energy in an internal combustion engine [7-11] and a fuel cell [12-14] in order to recycle it into useful forms such as electricity or power. However, hydrogen has a very low energy density by volume at room temperature and pressure condition. To compensate, hydrogen should be stored in gas phase at high pressure or in liquid phase. In order to solve the problem of low energy density by volume, a storage method using metal hydrides has been studied. However, there is a disadvantage that the energy density by mass is lowered when the metal hydrides are used to store hydrogen. As such, hydrogen has definite limitations in storability.

Ammonia is attracting attention as an energy storage medium that

can compensate for the disadvantages of hydrogen. When used as a fuel, ammonia does not produce carbon-related emissions such as CO_2, CO, and soot because it does not contain carbon in its molecular structure, just like hydrogen. In addition, there is little restriction on its feedstock because it can be produced from nitrogen and water which are abundant in nature using renewable energy. Ammonia shares the eco-friendly characteristics of hydrogen as an energy storage medium, but is far superior to hydrogen in storage stability [15]. In particular, since ammonia is in liquid phase at the condition of room temperature and 10 atm, it exhibits excellent storability and transportability. In the Fig 1. 2 [15], the economical comparison of hydrogen and ammonia is shown.

To utilize the ammonia as an energy storage medium, it is essential to develop a device to convert energy stored in the form of ammonia back to the usable form of energy such as electricity of power. For that purpose, in this study, the internal combustion engine, which is the one of the most widely used device for energy conversion and whose structural modification is easier than other device, selected for the energy conversion.

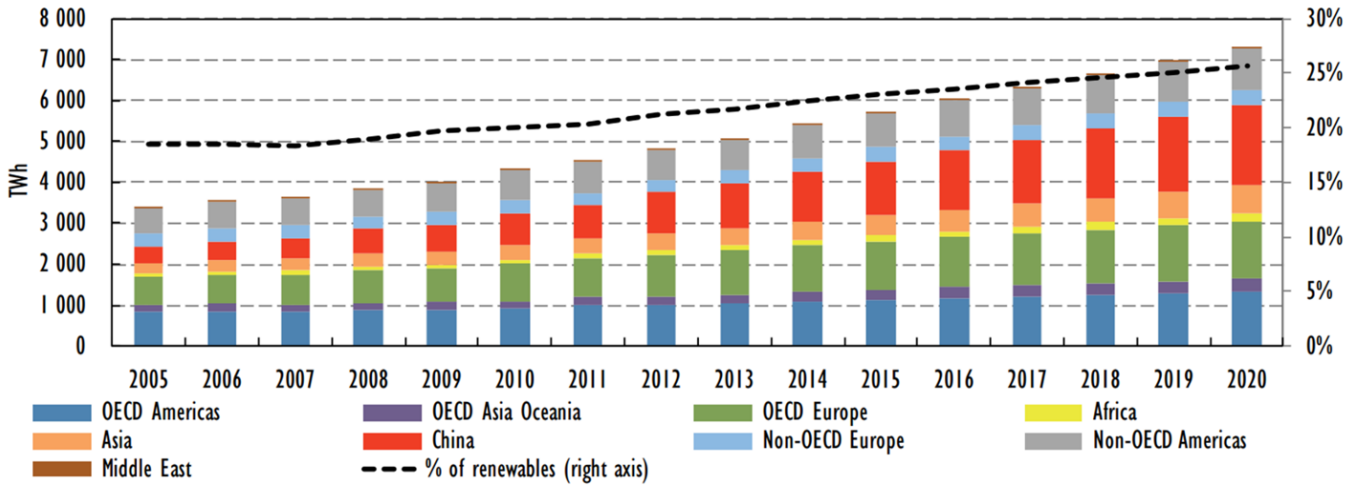

Figure 1. 1 Global renewable electricity production by region, historical and projected [1]

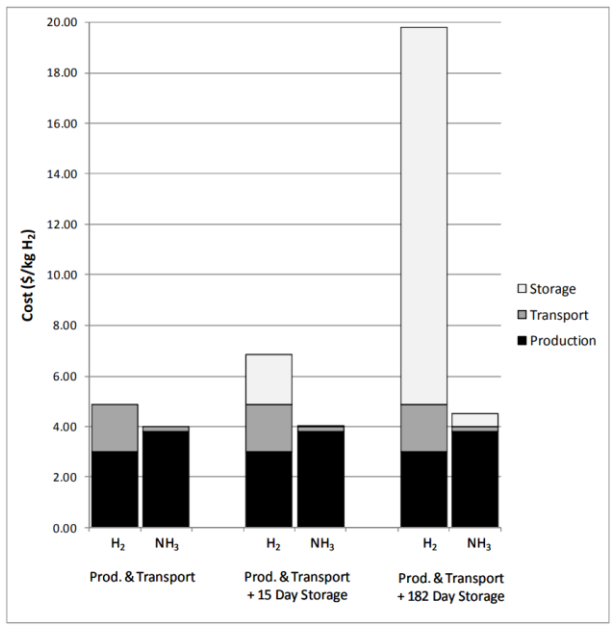

Figure 1. 2 Economical comparison of hydrogen and ammonia [15]

1.2 Characteristics of ammonia

Ammonia is a colorless gas with a characteristic odor, whose molecular formula is NH_3. Ammonia is harmful to the human body and it is corrosive to rubber and copper materials, so care is required. The vapor pressure at room temperature reaches about 8 atm and it evaporates easily. Because of its low molecular weight, it can spread easily into the air. However, since the self-ignition temperature is as high as 651 ° C, the risk of explosion when leaking is rather low.

Table 1. 1 compares the major properties of ammonia, which can be

affected the combustion, with diesel and gasoline, which are commonly used engine fuels. As can be seen in the table, ammonia has a very high latent heat of vaporization and high auto-ignition temperature, which means that it has very poor combustion characteristics. In addition, ammonia has a much lower energy content per unit mass than conventional engine fuels. However, the results are different when the energy content is compared for a stoichiometric fuel-air mixture. Eq. (1. 1) represents the chemical reaction of ammonia oxidation. The ratio of ammonia to air in the stoichiometric condition is relatively high because the number of hydrogen atoms per molecule is smaller than that of conventional hydrocarbon fuel. Therefore, when used as an engine fuel, there is no problem in terms of energy content. The poor combustion characteristics of ammonia should be overcome through the introduction of new combustion methods.

Table 1. 1 Comparison of properties related with combustion

	Boiling point (°C)	Latent heat of vaporization (kJ/kg)	Auto-ignition temperature (°C)	Energy content (MJ/kg-fuel)	Energy content (MJ/kg stoich. Mixture)
Diesel	280 ~ 340	230	256	41.4	2.76
Gasoline	30 ~ 220	305	280	44.0	2.83
Ammonia	-33.5	1371	651	18.6	2.64

$$NH_3 + 0.75(O_2 + 3.76N_2) \leftrightarrow 1.5H_2O + 3.32N_2 \qquad (1.1)$$

1.3 Previous researches

As previously mentioned, there have been many attempts to utilize ammonia as an energy storage medium through various studies. Particularly, researches on energy conversion device technology for ammonia, which is essential for the use of ammonia as an energy storage medium, have been concentrated on fuel cell and internal combustion engine, and contents are as follows.

1.3.1 Indirect use of ammonia as a fuel

The indirect use of ammonia as fuel is conducted by decomposition of ammonia into hydrogen. In order to overcome the disadvantages of ammonia, which shows relatively poor reaction characteristics compared to hydrogen, ammonia is decomposed into hydrogen and used in fuel cell where the hydrogen is widely used as fuel. Indirect use of ammonia has been studied mainly in proton-exchange membrane fuel cell (PEMFC), alkaline fuel cell and etc. TV Houdhary et al. [16] has studied the ammonia decomposition for fuel cell applications and confirmed the effect of the type of supported metal catalysts on the decomposition rate of ammonia. R Metkemeijer and P Achard [17] conducted experiments on the indirect use of ammonia and methanol for acid and alkaline fuel cells and compared the results. However, these methods require a temperature above 400 °C to produce hydrogen by decomposing

ammonia [18], and there is a disadvantage that efficiency loss is caused because a part of generated electricity is consumed to the decomposition.

1.3.2 Direct use of ammonia as a fuel

Owing to poor chemical reaction and combustion characteristics of ammonia, the devices that can be used for energy conversion where the ammonia is used directly as a fuel are somewhat limited. Since the operating temperatures of solid oxide fuel cell (SOFC) and internal combustion engine are relatively higher compared to other energy conversion devices, they are appropriate to use ammonia as a fuel, thus several studies have been conducted on these devices. Unlike the case of using ammonia indirectly in a PEMFC, SOFC does not require additional heating up for ammonia decomposition because the operating temperature reaches about 1000 K, and thus efficiency loss due to heating up does not occur. G Meng et al. [19] conducted a study on the use of ammonia in SOFC and compared the result for ammonia was compared with a result for hydrogen in the same experimental setup, which showed that power density of SOFC fueled by ammonia is slightly lower than that of SOFC fueled by hydrogen. In addition, some researchers have been studied on the reduction of NO produced during the operation of SOFC fueled by ammonia [20, 21].

Concentrating on the possibility of ammonia as a hydrogen-carrier, many studies have also been conducted to use ammonia as an internal

combustion engine fuel [22-36]. AR Reiter et al. attempted to burn the port injected ammonia by direct injection of diesel which is ignited at relatively low temperature than ammonia, and they could replace 40-80% of the energy with ammonia and achieved a reasonable fuel economy [27]. There are also a number of cases which used direct injection of mixture of ammonia and other fuel. CW Gross et al. [30] and K Ryu et al. [25] both investigated the direct injection of a mixture of ammonia and DME, and showed that ammonia can replace DME to some extent. However, as the ammonia ratio increased, the engine performance decreased and the emission of CO, unburned HC, soot, etc. increased due to the reduction of combustion temperature.

Studies on the use of ammonia as internal combustion engine fuel have also been performed in SI engines. SM Grannell et al. [32] and SO Haputhanthri et al. [29] have conducted a study on the use of gasoline and ammonia in a spark ignition engine. Both studies have been able to replace gasoline with ammonia in limited operating range, and using ammonia in certain operating range has shown better engine performance than gasoline alone. K Ryu et al. used direct injection of ammonia into a premixed gasoline-air mixture formed by port injection [23]. The power output of 2.7 kW was achieved by addition of ammonia injection to the baseline power of 0.6 kW by gasoline, and the brake specific CO decreased slightly. In addition, K Ryu et al. have also conducted studies to increase engine performance by using hydrogen dissociated from ammonia as an additional fuel [24]. Several attempts have also been made to use ammonia and hydrogen together in the SI engine to overcome the low flame speed of ammonia [22, 28, 34, 36].

In recent studies, most of them have applied dual fuel system to overcome the poor combustion characteristics of ammonia, and it is difficult to use ammonia as a sole fuel. Although studies were conducted in 1967 to operate compression ignition and spark ignition engines using ammonia as the sole fuel, they only succeeded in driving the engine under extremely limited operating conditions [31].

1.4 Objectives of study

The goal of this study is to develop a combustion strategy for internal combustion engine using only ammonia as a fuel to overcome the limitation of previous studies on internal combustion engine using ammonia as fuel. First, the combustion strategy for ammonia was proposed through the investigation of combustion characteristics of ammonia.

Modeling of the ammonia engine was performed to confirm the feasibility of the engine to which the proposed combustion strategy was applied. Detailed ammonia chemical reaction mechanism was used to further characterize the phenomena that occur under the operating of the ammonia engine. To compensate the increase in time cost by using detailed chemical reaction mechanism, the model was developed based on the quasi-dimensional modeling which can save the computing time and consider the physical characteristics of spray at same time.

combustion characteristics of the engine were confirmed and

analyzed through the simulation under various engine operating parameters. Emissions of NO should be particularly important because ammonia can produce NO through various reaction path, including thermal NO, though ammonia does not produce carbon-related emissions during the combustion process. A parametric study to confirm the NO emission characteristics of the engine with the combustion strategy proposed was also conducted and the NO production mechanism under the ammonia combustion strategy was analyzed based on the simulation results.

Chapter 2. Methodology

2.1 Combustion strategy for ammonia engine

The newly proposed ammonia combustion strategy in this study is schematically shown in Fig 2. 1 During the intake process, a small amount of ammonia (φ=0.1–0.3) is injected, and the injected ammonia is mixed with the air inside the cylinder to form a homogeneous lean mixture. The lean mixture is auto-ignited during the compression process, increasing the internal temperature and pressure of the cylinder to such an extent that it is possible to burn the main spray of the ammonia. The main injection of ammonia starts either before or after the auto-ignition of the lean mixture (hereinafter referred to as 'pre-combustion') and ammonia spray combustion occurs. Through the implementation of this combustion strategy, it is possible to overcome the limitation of compression ignition due to the high auto-ignition temperature of ammonia.

Hereafter, the term 'pilot injection' is used to refer to small amount of ammonia injection during the intake process. Unlike the term 'pilot injection' used in modern diesel-fueled engine, which is used typically to reduce combustion temperature or pressure, 'pilot injection' in this proposed strategy is intended to raise the in-cylinder temperature and pressure for ammonia spray combustion through pre-combustion process.

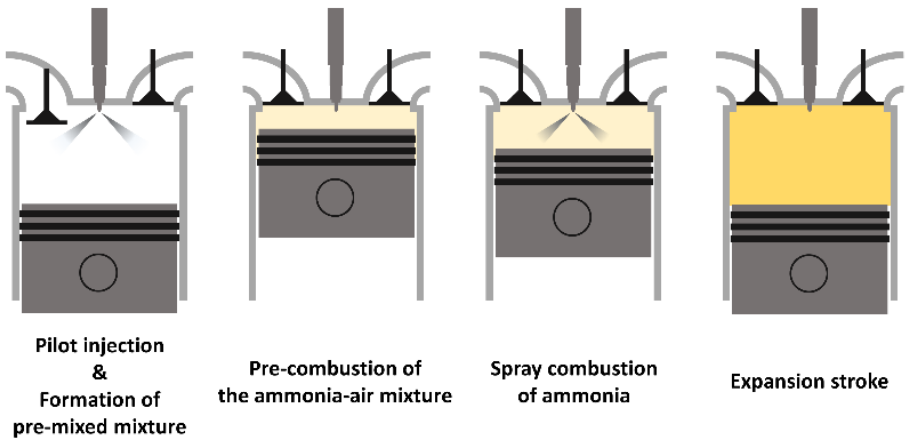

Figure 2. 1 New combustion strategy for ammonia

The pre-combustion of lean ammonia-air mixture formed by pilot injection of ammonia can be realized through the unique ignition delay characteristics of ammonia, which are very different from conventional hydrocarbon fuels. Fig 2. 2 shows the result of simulation on ignition delay of ammonia at different equivalence ratios under fixed volume and the conditions of 1300 K and 70 bar using ammonia chemical reaction mechanism developed in this study, which will be introduced in following section 2.2.3. Ammonia shows the shortest ignition delay at an equivalence ratio of approximately 0.4, and there is no significant difference in the ignition delay compared to the equivalence ratio of 1.0, even at the equivalence ratios of 0.1. The tendency is also consistent with the experimental result by Mathieu et al. [37]. With this constant-volume ignition delay characteristics of ammonia, it is expected in the proposed engine operation that leaner ammonia-air mixture would pre-combust more easily due to less charge cooling caused by smaller amount of

direct-injected pilot fuel and lower specific heat ratio of leaner ammonia-air mixture.

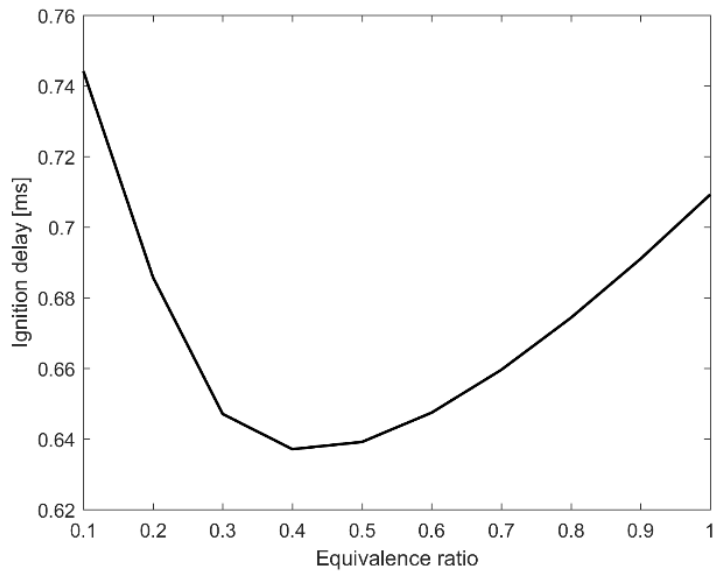

Figure 2. 2 Unique ignition delay characteristics of ammonia

Therefore, by using pre-combustion of a leaner ammonia–air mixture to further increment the temperature and pressure of the geometrically compressed mixture, it is possible to overcome the compression limit from engine hardware. In this way, the stable operation of the ammonia spray combustion is possible, where the remaining oxygen after the pre-combustion is used.

2.2 Model description

The engine modeling was performed to verify the feasibility of the proposed combustion strategy and to con-firm the operating characteristics of such engine. An ammonia chemical reaction mechanism, which is modified from the mechanism developed by Mathieu et al. [37], has been used to accurately predict the pre-combustion and main combustion of the ammonia–air mixture as well as the NO emission, which are the major parts of the proposed strategy regarding reaction chemistry. The modeling was performed based on a quasi-dimensional model to compensate for the increased time cost through the use of comprehensive chemical reaction mechanisms, while simultaneously taking into ac-count the physical properties of the spray.

2.2.1 Modeling scope and major assumptions

The basic assumptions introduced in the engine modeling are as follows. The simulation is performed during the period from the intake valve closing (IVC) timing to exhaust valve opening (EVO) timing. The ammonia injected during the intake process (pilot injection) is assumed to be fully vaporized with charge cooling and uniformly mixed with intake air until the IVC over a sufficient period of time; thus, the simulation starts with compressing the homogeneous, lean ammonia-air mixture at the IVC. The inside of the cylinder is divided into one ambient zone and several user-

definable fuel spray zones from the start of main injection near the compression end, assuming that the thermodynamic properties in each zone are uniform. The ambient zone consists of the lean mixture of pilot-injected ammonia and air entering during the intake process or products resulting from the pre-combustion of the lean ammonia–air mixture. It is also assumed that only the gas phase species can participate in the reactions occurring in the cylinder.

2.2.2 Spray model

The spray model used for the engine modeling is based on a packet spray model by Hiroyasu et al. [38]. Fuel spray consists of many sub-spray zones divided into the axial direction, which is the direction of spray penetration, and the radial direction, which is perpendicular to axial direction. Fig 2. 3 shows a schematic diagram of spray with ‘n’ zones in the axial direction and ‘m’ zones in the radial direction. At the start of injection (SOI) timing, the injected fuel is distributed with the same amount in each radial zone. The injected fuel is distributed in the axial direction fuel zone according to the pre-defined finite time interval. It is noted that the original Hiroyasu's model generates new zones in the axial direction at every time step, but the time cost will be significantly increased if this approach is used with the detailed chemical reaction mechanism.

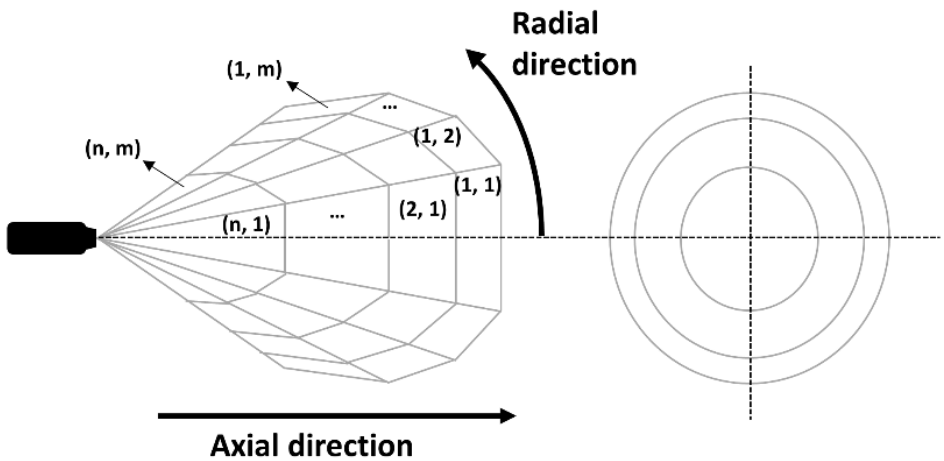

Figure 2. 3 Schematic diagram of spray model

The spray development in each fuel zone proceeds along the penetration. In this study, the correlation proposed by Hiroyasu et al. [38] is used to obtain the penetration of spray injected, and the equations are as Eq. (2. 1) ~ (2. 3). The correlations of spray penetration are different before and after break-up time. According to Eq. (2. 1), penetration increases in proportion to time, since it is assumed that the velocity of the spray is constant until break-up time. After the break-up time, atomization and evaporation of the fuel spray starts and the air flow into the spray area occurs and the speed of the spray tip decreases with time, which is expressed through Eq. (2. 2). Correlation of break-up time is expressed in Eq. (2. 3), and penetration and spray speed decrease by increasing interaction with the outside air as it goes to the outside of spray, which is realized through Eq. (2. 4). Slower spray speed of peripheral spray zones than the spray speed of inner spray zones by the interaction with the ambient is implemented with Eq. (2. 4).

$$S = 0.39\sqrt{\frac{2\Delta P}{\rho_l}}t \qquad (0 < t < t_{bu}) \qquad (2.\ 1)$$

$$S = 2.95\left(\frac{\Delta P}{\rho_a}\right)^{\frac{1}{4}}\sqrt{d_n t} \qquad (t_{bu} \le t) \qquad (2.\ 2)$$

$$t_{bu} = 28.65\frac{\rho_l d_n}{\sqrt{\rho_a \Delta P}} \qquad (2.\ 3)$$

$$\mathrm{S}_R = \mathrm{S}_{CL}\exp[-0.6947\left(\frac{R-1}{R_{max}-1}\right)^2] \qquad (2.\ 4)$$

The mixing of the ambient and spray is explained by the momentum conservation. The amount of air entrainment into the spray zone can be obtained from Eq. (2. 5). $u(t)$ in Eq. (2. 5) can be obtained by differentiating Eq. (2. 1) and Eq. (2. 2) over time. The decelerate of the spray zone increases toward the outside of the spray zones due to more interaction with ambient, which results in the more air entrainment into the outside of the spray area as expressed in Eq. (2. 5).

$$\mathrm{m}_f u_0 = (m_f + m_{a,ent})u(t) \qquad (2.\ 5)$$

2.2.3 Chemical reaction model

In this model, the detailed ammonia chemical reaction mechanism is used to model the entire chemical reaction occurring inside the ammonia engine. In the proposed combustion strategy, various phenomena such as pre-

combustion of lean ammonia-air mixture, spray combustion of ammonia, and generation of NO through various pathways, which are the main pollutant arising from such a combustion process, occur through chemical reactions. By using the detailed ammonia chemical reaction mechanism, it is possible to accurately predict the pre-combustion which is mainly kinetically driven. In addition, the physical and chemical characteristics of the spray combustion can be realized by using the ammonia chemical reaction mechanism together with the packet spray model. In the ammonia engine, NO can be generated from the fuel-bound nitrogen in addition to the thermal NO generated under the high temperature and pressure condition in the conventional engine. In the relatively low temperature condition near 1000 °C or in the very ammonia-rich spray region, NO may be reduced through the reaction with ammonia. Using the ammonia chemical reaction mechanism, it is possible to effectively predict the amount of NO by considering both the NO production and the consumption pathway.

The ammonia chemical reaction mechanism used in this study is a modification of the chemical reaction mechanism developed by Mathieu et al. [37], which considers 35 species and 159 chemical reactions. Mathieu et al. has developed a chemical reaction mechanism based on the chemical reaction mechanisms by Dagaut et al. [39], which can predict the delay of ammonia ignition over a wide range of temperature (1560 ~ 2455 K) and pressure (1.5, 11, 30 atm) conditions. However, the developed mechanism has a disadvantage in that the prediction performance of the thermal deNOx process, which is a reduction of NO by ammonia as a reagent at around 1000 °C, is degraded.

Replacing the reaction rate coefficients of $NH_2 + NO_2 \leftrightarrow N_2O + H_2O$, $NH_2 + NO_2 \leftrightarrow H_2NO + NO$ and $NNH + O_2 \leftrightarrow N_2 + HO_2$ with that from Klippenstein et al. [40] and $NH + NO \leftrightarrow N_2O + H$ with that from Miller et al. [41], the predictability of the ignition delay can be maintained at a similar level while improving the thermal deNOx prediction performance. Fig 2. 4 shows the results of thermal deNOx experiments in a flow reactor from the study of Kasuya et al. and Fig 2. 5. (a) and (b) show thermal deNOx simulations using the mechanism from Matieu et al. before and after the improvement at the same simulation condition in Fig 2. 4. The simulation results using the ammonia chemical reaction mechanism obtained by the improvement of the mechanism by Mathieu et al. show that the temperature window of thermal deNOx process in most oxygen concentration conditions is extended to the low temperature part, being close to the result from experiment.

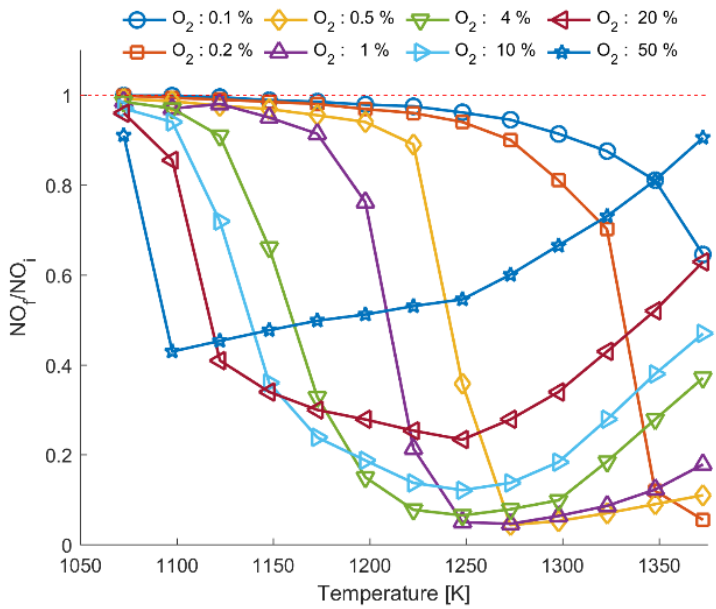

Figure 2. 4 Experiment result from Kasuya et al. [42]

Inlet concentration: NO = 500 ppm, NH3 = 1000 ppm, H2O = 5 %, balance N2.

Residence time 88.0/T s (T in Kelvin)

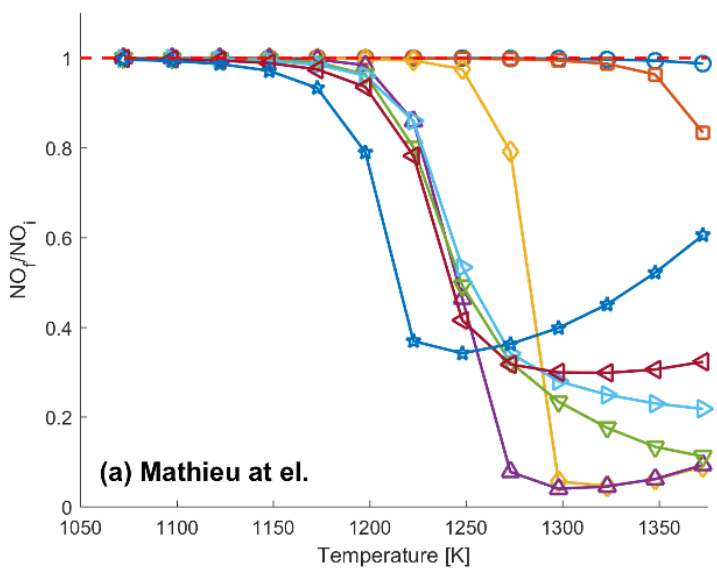

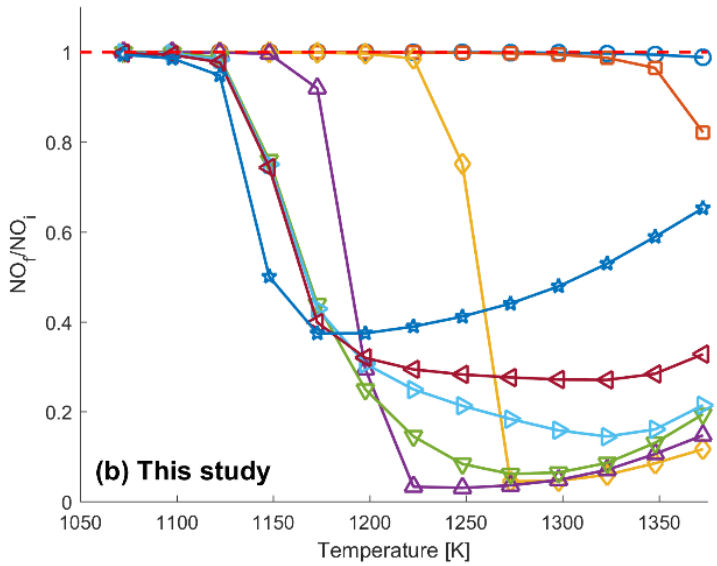

Figure 2. 5 Results of thermal deNOx simulation (a) with mechanism developed by Mathieu at el. and (b) with mechanism developed in this study

2.2.4 Thermodynamics model

To evaluate the thermodynamic states of multi-zone including ambient zone and multiple fuel zones, the following ordinary differential equations are solved at each time step. In this model, temperature and species are solved separately for each zone, while it is assumed that the pressure is uniform throughout the cylinder. Eq. (2. 6) is the ideal gas law, where P, V, and n are pressure, volume and the number of moles in each zone, respectively, and R is the universal gas constant. Eq. (2. 7) is the first law of thermodynamics, where c_v is the specific heat at the constant volume and m_i, u_i, and h_i are the

mass, internal energy and the enthalpy of each species, respectively, and Q_{HT} is the amount of heat transfer. m_f and h_f are the mass and the enthalpy of fuel. The contribution of chemical reaction to the second term on the left hand side (internal energy change rate by number of moles change in chemical reactions) is calculated by Cantera toolbox within MATLAB using aforementioned chemical reaction mechanism. Hohenberg's correlation [43] is adopted for heat transfer calculation, which is in expressed in Eq. (2. 8). The simplified area for the heat transfer is calculated by assuming that in-cylinder volume is cylindrical. Eq. (2. 9) represents the volume constraint, where V_i is volume of each zone. The change rate of total cylinder volume in Eq. (2. 9) is calculated by Eq. (2. 10) where B, a and l are bore, radius of crank and connecting rod length, respectably.

$$\dot{P}V + P\dot{V} = \dot{n}RT + nR\dot{T} \qquad (2.\ 6)$$

$$mc_v\dot{T} + \sum \dot{m}_i u_i + P\dot{V} = \dot{Q_{HT}} + \dot{m}_f h_f \qquad (2.\ 7)$$

$$\dot{Q_{HT}} = h_g A\left(T_g - T_w\right),\ where \quad h_g = \alpha_s V^{-0.06} P^{0.8} T^{-0.4}\left(\overline{s_p} + b\right)^{0.8} \qquad (2.\ 8)$$

$$\dot{V} = \sum \dot{V}_i \qquad (2.\ 9)$$

$$\dot{V} = \frac{\pi}{4} B^2 a\dot{\theta}\left(sin\theta + \frac{asin\theta cos\theta}{\sqrt{l^2 - a^2\, sin^2\,\theta}}\right) \qquad (2.\ 10)$$

There are 2i+1 unknowns in above equations, which are volume and temperature of each zone and cylinder pressure which is uniform throughout the cylinder, and by solving 2i+1 equations together thermodynamic state of

each zone can be calculated.

2.2.5 Simulation parameters

Simulation of the engine using the proposed ammonia combustion strategy was performed using the model developed. The parameters used in the simulation are shown in Table 2.1.

Table 2. 1 Engine parameters for simulation

Engine type	4-stroke
Bore	83.0 mm
Stroke	92.0 mm
Con. rod length	145.8 mm
RPM	1000
Injection pressure	500 bar

The Engine parameters refer to the D-engine from Hyundai-Motor Group. Because the D-engine is an undersquare type whose stroke is longer than its bore, it is relatively easy to implement a high compression ratio to achieve proper combustion timing of ammonia. Because the atomization of ammonia is considered to occur easily owing to its high vapor pressure, it might

be possible to increase the flow rate of the fuel injection by using a larger nozzle size than typical diesel injector. In this study, the specification of Bosch HDEV GDI injector was adopted for high pressure fuel injection. It was also considered that the use of GDI injector in the implementation of the experimental engine might be more suitable for low viscosity of ammonia. The present state-of-the-art injection pressure in a commercial GDI injector was 500 bar, which was used in our simulation.

Applying the proposed combustion strategy could mitigate the initial intake temperature condition where the ammonia internal combustion engine can operate only with direct injection, but the intake temperature and compression ratio that enable the operation of engine with proposed ammonia combustion strategy was still in high level. Before the parametric study, intake temperature and compression ratio to be used in the subsequent simulation were set first. Compression ratios have limitations that can be increased due to the limit of physical machining, unlike intake temperature, and it is also difficult to change if the engine geometry is determined once. Therefore, in this study, the engine parameters for the simulation were set by assuming the maximum value of the intake temperature which can be elevated assuming the use of heat exchanger, and setting the compression ratio to obtain a sufficient operating region at a given intake temperature condition.

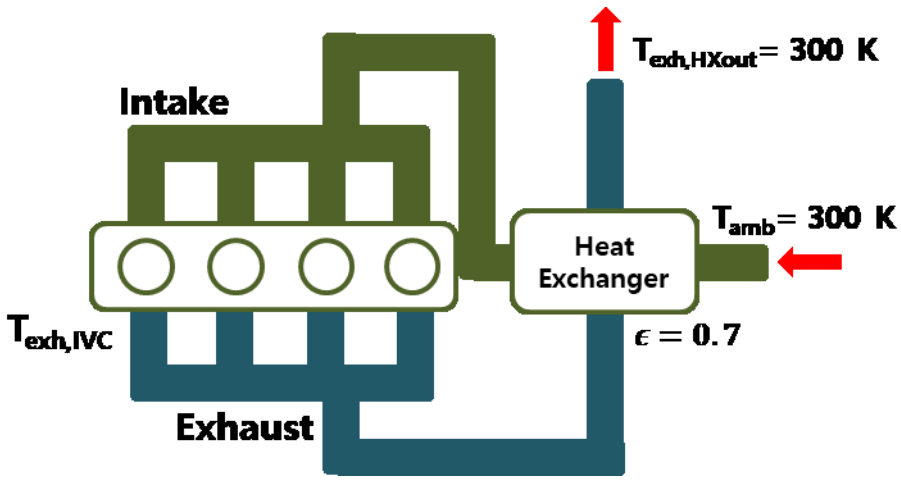

Figure 2. 6 Schematic diagram of engine and heat exchanger

Fig 2. 6 is a schematic representing the engine and heat exchanger. $T_{exh,IVC}$ were assumed to be in the range of 600 to 800 K, $T_{exh,HXout}$ and T_{amb} were assumed to be 300 K, respectively, and then T_{intake} was calculated. Assuming that the effectiveness of heat exchanger is 0.7, the range of T_{intake} obtained from the calculation is about 240 ~ 340 K. Considering the heat transfers between cylinder and heat exchanger, it can be expected that an intake temperature of at least 200 ℃ can be obtained. We set the intake temperature at 200 °C and increase the compression ratio from 15 at the equivalence ratio of 0.6, which is a mid-low load condition. Compression ratio conditions up to 30 showed efficiency of less than 90% for all start of main injection (SOI) timing condition. Figure x shows the change of $IMEP_g$ according to the SOI timing at the compression ratio of 35 with intake temperature of 200 °C. The result with ϕ_{pilot} of 0.2 shows an operable SOI timing range of 10 CAD, while the result with ϕ_{pilot} of 0.3 shows operable SOI timing range as narrow as 4

CAD. In the narrow SOI timing range, it is considered that it is difficult to grasp the change of the engine operating characteristics according to SOI timing change. Therefore, the intake temperature of 220 °C which is the temperature increased by 20 °C from the intake temperature condition of Fig 2. 7 and the compression ratio of 35 was set as the engine parameters for the simulation and the subsequent parametric study was performed.

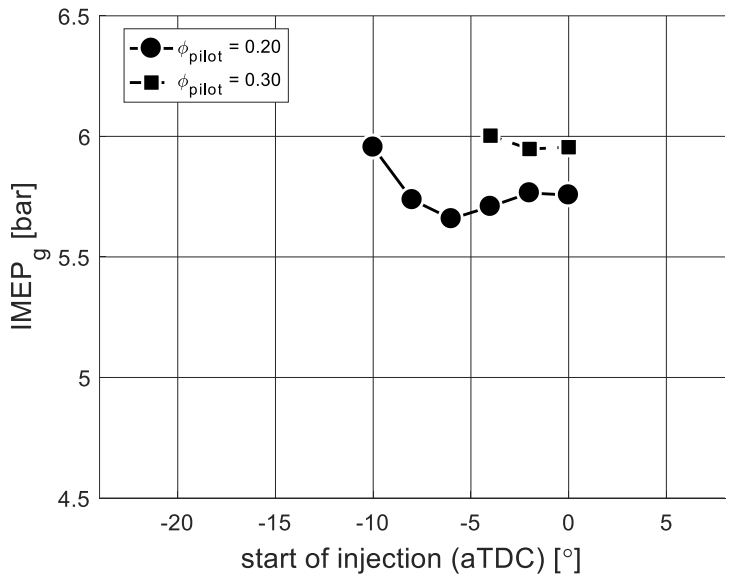

Figure 2. 7 IMEPg under different SOI timing and amount of pilot injection

(compression ratio = 35, Tintake = 200 °C)

In order to investigate the influence of the number of grid, the number of grids is changed for a typical operating condition and the effects of number of grids on $IMEP_g$ and NO emission are shown in Fig 2. 8 and Fig 2. 9. $IMEP_g$ is not that changed depending on the number of grid, but the

emission of NO is rather affected by the number of grid, and the value is saturated as the number of grid increases. Here, the influence of the number of grid on NO emission is caused by more detailed temperature distribution according to the increased number of grid.

In this model, modeling analysis is performed based on 4 radial directions and 4 axial directions. With 4 grids in each direction, NO results with little difference from the saturated NO value for increased number of grid could be obtained and at the same time, the complexity of the system to be analyzed has been reduced, and the time cost has been saved

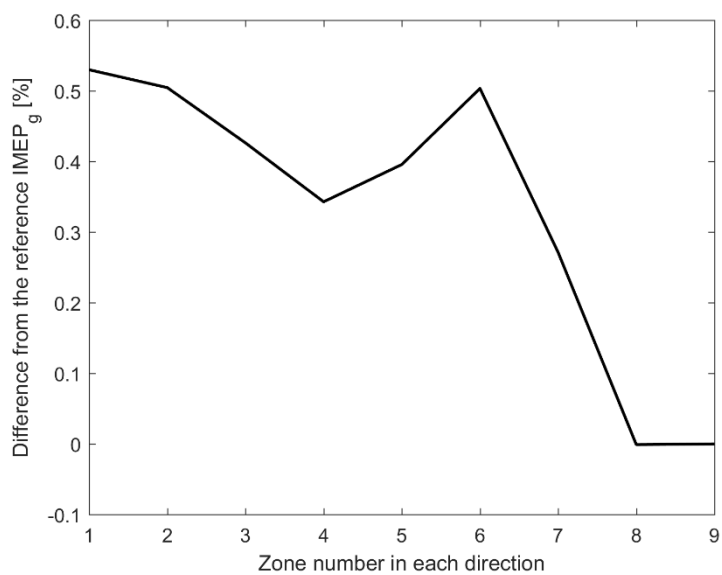

Figure 2. 8 IMEPg difference from the reference data (9×9 grids) at different number of grids

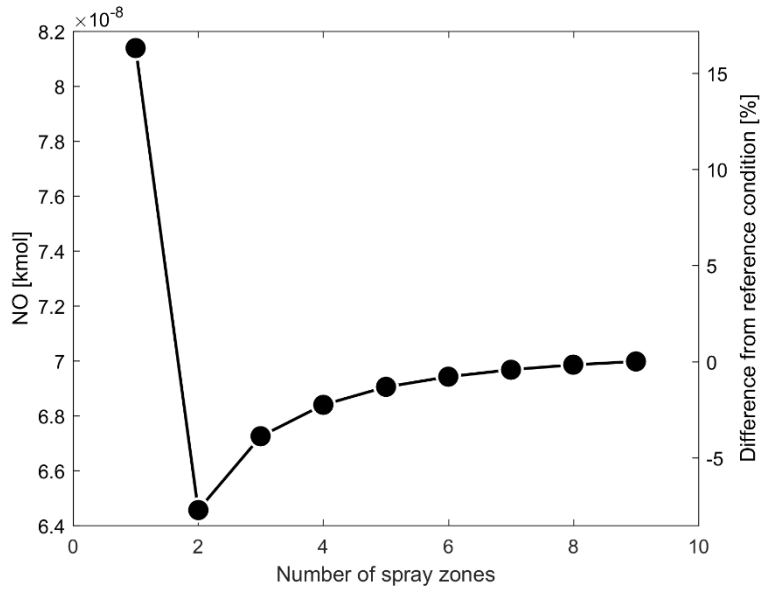

Figure 2. 9 NO with different number of grids in radial and axial direction

Chapter 3. Operating characteristics of the engine with ammonia combustion strategy

3.1 Pre-combustion of ammonia-air mixture

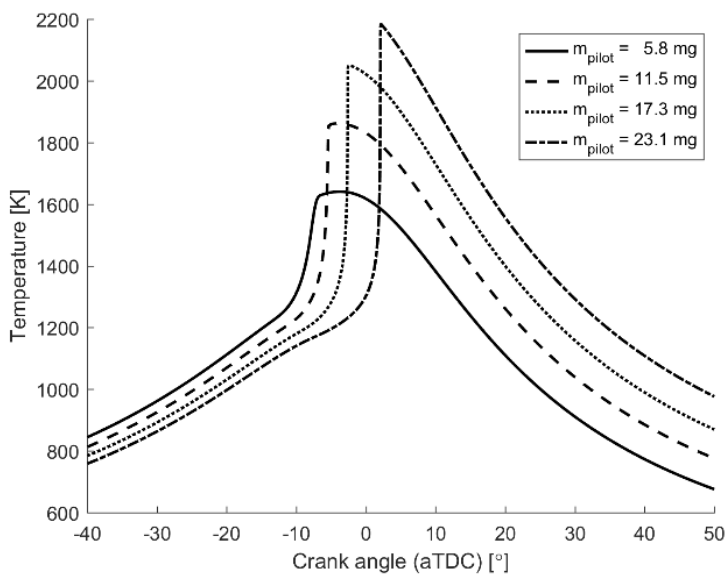

Figure 3. 1 Temperature profile of pre-combustion with different amount of fuel used in pilot injection

In this section, the results will be presented for the pre-combustion of lean ammonia-air mixture by pilot injection. As mentioned earlier, it is assumed that the pilot injection occurs during the intake process and the pilot-injected ammonia is sufficiently mixed with the intake air until the intake valve closing timing to form homogeneous ammonia-air mixture; therefore, only the

amount of pilot injection was considered as a simulation parameter.

Fig 3. 1 is a graph depicting the temperature profiles of the pre-combustion of a lean ammonia–air mixture with various amount of ammonia injected in the pilot injection. Too early pre-combustion can increase the negative work during the compression process; meanwhile, if pre-combustion is too late, it may misfire because of charge cooling by the overlapped main injection spray or the piston expansion. Therefore, in the given engine geometry and pilot injection quantity conditions, the simulation was performed by setting the intake air temperature to 220 °C, such that the pre-combustion would occur in the range from −10 crank angle degree (CAD) after top dead center (aTDC) to TDC. The pilot injection quantities used in the simulation were 5.8, 11.5, 17.3, and 23.1 mg/cycle (hereafter just 'mg' is used instead of mg/cycle), which correspond to equivalent ratios of 0.1, 0.2, 0.3, and 0.4 at a given intake condition.

As shown in Fig 3. 1, the auto-ignition of the premixed mixture of pilot-injected fuel and air can be observed, and the timing of the auto-ignition is delayed as the pilot injection quantity increases. In this operating condition, the auto-ignition did not occur, owing to a longer ignition delay with pilot-injected fuel more than 23.1 mg. The ignition delay, which was increased with more pilot-injected fuel, could be attributed to the combined effect of the decrease in the specific heat ratio due to the increase in the ammonia proportion in the ammonia-air mixture, the reduction in the temperature of the ammonia–air mixture due to the increase in the charge cooling with more ammonia, and the ammonia ignition delay characteristics previously discussed. As can be

seen in Fig 3. 1, as the pilot-injected fuel increases, the pre-combustion timing delays, but at the same time, the maximum temperature in the cycle increases by the pre-combustion.

In order to compensate for the high latent heat of evaporation of the following main injection of ammonia for spray combustion, a sufficiently high temperature inside the cylinder is required. Therefore, a larger pilot injection amount is favorable. However, if the pre-combustion is delayed too much owing to the increased amount of pilot injection and the main injection may start before the occurrence of the pre-combustion, misfire of the pre-combustion may occur owing to the charge cooling by the main injection of ammonia. Therefore, it can be considered that there will be an appropriate amount of pilot injection and a proper SOI timing of the main ammonia spray for every engine operating condition.

In this section, we describe the simulation performed on the condition with the pilot injection up to 23.1 mg. However, the pre-combustion occurs after the TDC with 23.1 mg of pilot-injected fuel, which is considered too late and will be easily overlapped by the start of injection (SOI) timing of the main ammonia spray (hereinafter referred to as 'SOI timing'). As described above, when the SOI timing overlaps with the pre-combustion, the pre-combustion may be delayed or even misfired by charge cooling effect of the main spray, and thus the stability of the engine operation may deteriorate. Therefore, the amount of pilot injection in the following sections was limited to a maximum of 17.3 mg (or equivalence ratio of 0.3 for pre-mixed ammonia and air mixture).

3.2 Influence of SOI timing on engine performance

This section discusses changes in combustion mode and efficiency with varying injection quantities and SOI timings. The following comparison was made to consider the various injection strategies that can be applied to actual engine operation.

Fig 3. 2 shows the changes in the pressure profile at different SOI timings as the amount of pilot injection and main injection is equal to 11.5 mg. The simulation was performed at 4 CAD intervals from the SOI timing of −24 CAD aTDC to 8 CAD aTDC. It is noted that only the simulation conditions with higher than 90% combustion efficiency are included in the results. As can be seen from Fig 3. 2, the results with SOI timing of 4 CAD aTDC and 8 CAD aTDC were excluded owing to low combustion efficiency caused by delayed SOI timing after the TDC.

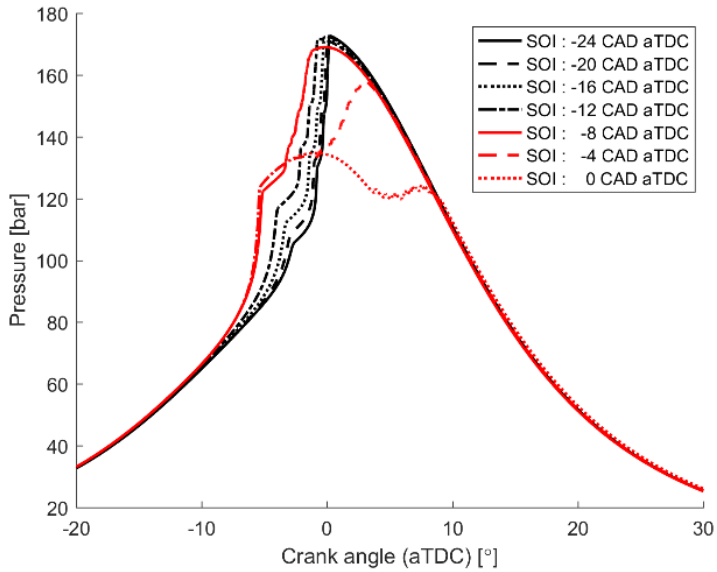

Figure 3. 2 Pressure profile of ammonia engine under various SOI timing

When the SOI timing is advanced before -4 CAD aTDC, it can be seen that the timing of pre-combustion is retarded as the SOI timing is advanced due to the cooling of the cylinder due to the latent heat of evaporation of the ammonia main injection. In addition, with the advanced SOI timing, the amount of lean ammonia-air mixture entrained into the spray zone is increased and the amount of lean ammonia-air mixture in the ambient zone, which causes pre-combustion, is relatively reduced, therefore, the increase in temperature and pressure by pre-combustion is reduced. As a result, if the SOI timing is advanced, the spray combustion occurs in the form of a partially pre-mixed combustion, which occurs after the long mixing time of spray, with little or no assistance from the pre-combustion. Fig 3. 2 shows that the timing of pre-combustion is delayed with advanced SOI timing. For relatively late SOI

timing (-4, 0 CAD aTDC) where ammonia injection does not affect pre-combustion (occurring near -4 CAD aTDC), it can be seen that the timing of ammonia spray combustion is also delayed with delayed SOI timing like the spray combustion trend in typical diesel engines. Fig 3. 3 shows the trend of the combustion timing for various SOI timing in different way. The CA50 in Fig 3. 3 shows the crank angle at which the cumulative heat release for the ammonia main injection is 50% and the cumulative heat release includes the heat release of fuel from the lean ammonia-air mixture in ambient zone. This trend of combustion is also observed under different operating conditions of the ammonia combustion strategy proposed in this study. If the SOI timing is further advanced, the cylinder homogeneity near the TDC is increased and the combustion phase becomes similar to the combustion in the HCCI engine. This phenomenon can occur only in low load conditions because it appears in the situation where the fuels from the pilot and main injection burns together in the form of premixed combustion without the support of pre-combustion and, as shown in Fig 3. 2, misfire occurs with the amount of fuel in lean ammonia-air mixture which exceeds a certain amount. For this reason, we excluded the combustion in the mode of HCCI from consideration in the discussion below.

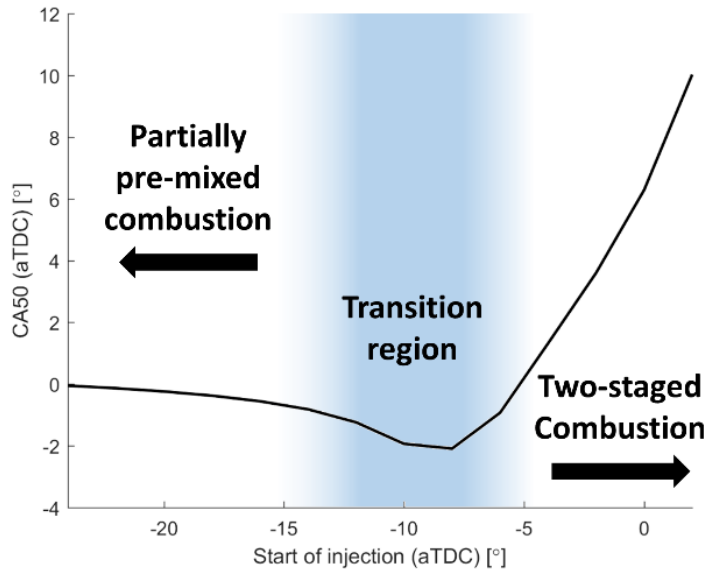

Figure 3. 3 Change of combustion mode according to SOI timing

3.3 Engine performance under varying ratio of pilot and main injection with fixed amount of total fuel used

In order to confirm the operating characteristics of the ammonia engine according to the ratio of the pilot injection amount and the main injection amount, the conditions with pilot injection amount of 5.8 mg and 17.3 mg was additionally simulated, while total fuel consumption amount was maintained at 23.1 mg. The ratio of the pilot injection to the main injection at this time is 1: 3 and 3: 1, respectively. The simulation results are shown in Fig 3. 4 and 3. 5.

The change in combustion behavior with the variation of SOI timing is similar to the result with the pilot injection amount of 11.5 mg as shown in Fig 3. 2. In the range where the latent heat of evaporation of the main injection affects the pre-combustion, the timing of spray combustion is delayed with the advanced SOI timing, and in the range where the main injection does not affect the pre-combustion, the spray combustion timing is also advanced when the SOI is advanced. For reference, as shown in Fig 3. 1, when the fuel is injected only through pilot injection without main injection the timing of pre-combustion was -8 and -3 CAD aTDC for 5.8 mg and 17.3 mg respectively.

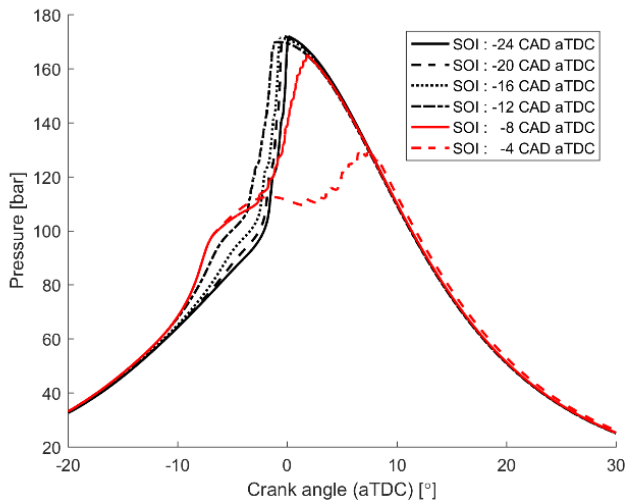

Figure 3. 4 Pressure profile with varying SOI timing under the condition with pilot injection of 5.8 mg and main injection of 17.3 mg

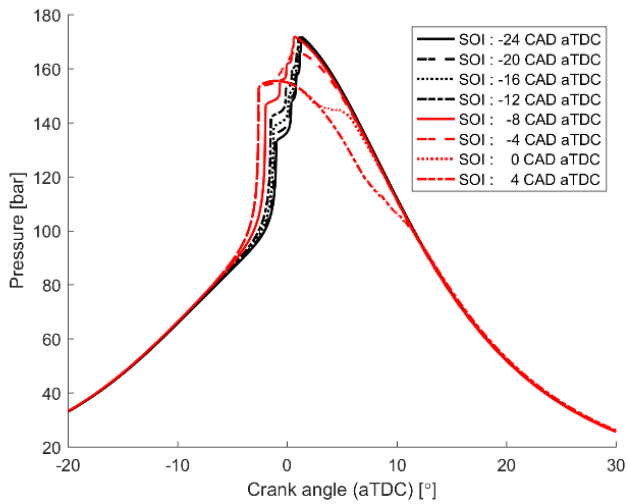

Figure 3. 5 Pressure profile with varying SOI timing under the condition with pilot injection of 17.3 mg and main injection of 5.8 mg

Although the overall trend of combustion is similar, the timing of pre-combustion and the heat release vary depending on the ratio of the pilot injection to the main injection, resulting in a difference in the thermal efficiency of the cycle and operable SOI timing range. This can be seen in Fig 3. 6 which shows the change of $IMEP_g$ at different SOI timing and pilot injection quantity. This included the results of Fig 3. 2 where the amount of pilot injection is 11.5 mg.

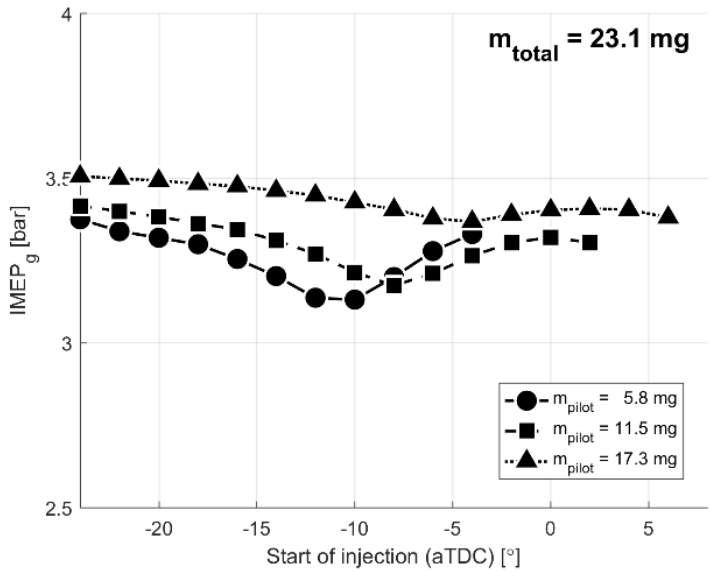

Figure 3. 6 IMEPg under different SOI timing and ratio of pilot injection to main injection with fixed total amount of fuel used

First, the Fig 3. 6 shows the change in the operable SOI timing range according to the pilot injection amount for a given total fuel input (23.1 mg) for a cycle. As can be seen in Fig 3. 1, it is possible to burn the fuel from main injection even when the main injection timing is significantly advanced to the point before the timing of pre-combustion, or when the mode of combustion is similar to HCCI. However, the right limit of the operable SOI timing range is extended as the amount of pilot injection increases. This is because as the amount of fuel used for pilot injection increases, the temperature after pre-combustion increases and the high temperature required for combustion of ammonia main spray last longer. With fixed amount of total fuel, the charge cooling effect is reduced by the main injection amount decreased with the increase of the pilot injection amount, which also contributes to the expansion

of the operable SOI range timing.

The $IMEP_g$ graph has a shallow V shape. The shape is caused by the change of compression work due to pre-combustion, change of expansion work and heat transfer by combustion of main injection. To understand this, Fig 3. 7 graphically shows the compression work, expansion work, and heat transfer changes with various SOI timing as the pilot injection and main injection amounts are equal to 11.5 mg (case in Fig 3. 2). On the left side of the graph, work or heat transfer is indicated. On the right side, the difference is shown based on the value at -8 CAD aTDC, which represents the peak value in each case of expansion work, compression work, and heat transfer.

Negative work during the compression process is greatly influenced by the timing of pre-combustion. As can be seen in Fig 3. 7, for the SOI timing before -8 CAD aTDC where main injection does not affect the pre-combustion, the earlier the SOI timing is, the more delayed the pre-combustion is. For the SOI timing delayed more than -8 CAD aTDC, the negative work during compression is almost constant because the timing of the pre-combustion is constant regardless of the SOI timing. At the SOI timing of -8 CAD aTDC, which is the boundary between the region where the main injection affects the pre-combustion and the region where it does not, the peak temperature due to the spray combustion occurs closest to the TDC, and the expansion work decreases due to the increase of the heat transfer amount. Under typical diesel engine operating conditions, as the peak pressure approaches the TDC, the expansion becomes higher. However, under the present engine geometry and the condition of high intake temperature of 220 °C, the heat transfer becomes

dominant, leading to the results obtained. As the SOI timing is delayed more than -8 CAD aTDC, CA50 approaches to 5 ~ 10 CAD aTDC which is the optimum range of SOI timing in a typical diesel engine, thus, the heat transfer amount decreases and the expansion work increases. As a result, the $IMEP_g$ has a pointed shape downward.

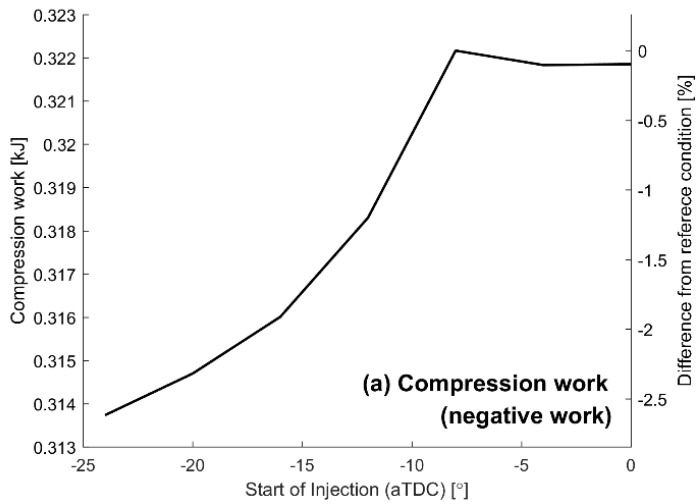

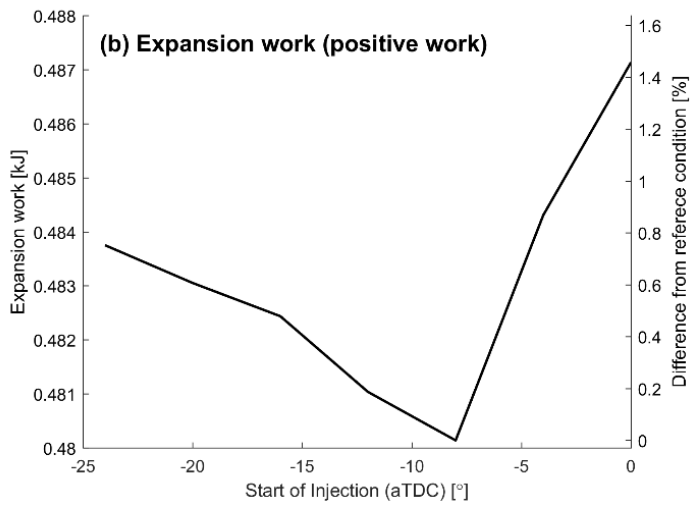

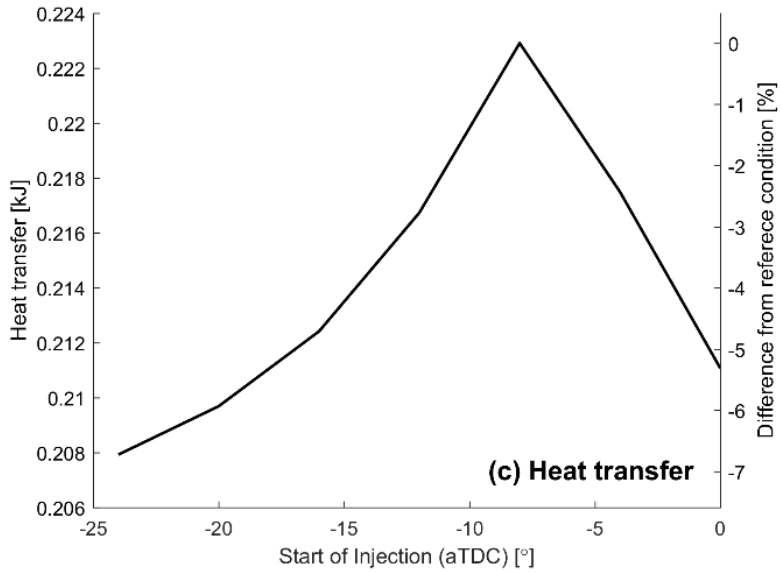

Figure 3. 7 Compression work, expansion work and heat transfer at various SOI timing

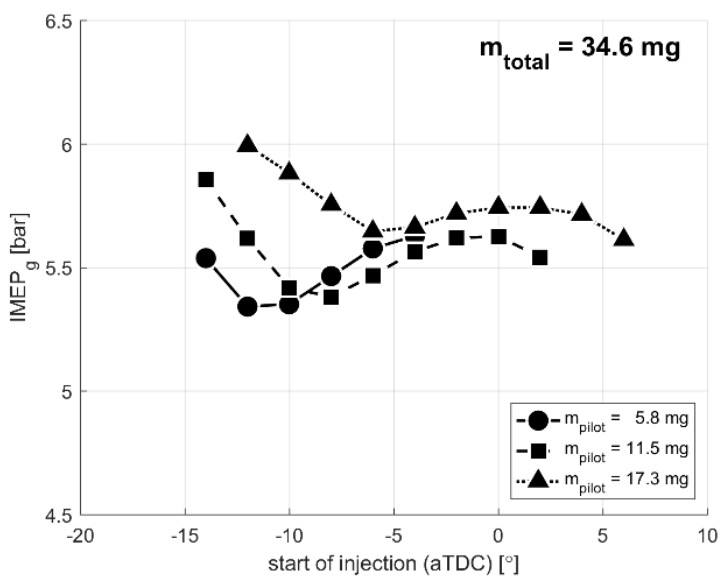

Figure 3. 8 $IMEP_g$ change according to SOI timing and ratio of pilot and main injection

Fig 3. 8 shows changes in $IMEP_g$ at different SOI timing and amount of pilot injection when the total fuel used is 34.6 mg. Unlike the case where the total fuel amount is 23.1 mg, it can be confirmed that the combustion is no longer stably performed when the SOI timing is too early (-20 to -16 CAD aTDC) under most conditions. This is because the condition of temperature and pressure to burn the ammonia main spray was not achieved by pre-combustion due to decreased amount of lean ammonia-air mixture, which is caused by extended duration of main injection with increased amount of main injection, leading to increase of spray mixing time. When the pilot injection quantity is small, the SOI timing can be slightly advanced as compared with the case where the amount of pilot injection is large since the pre-combustion timing is relatively early. On the contrary, the peak temperature due to pre-combustion is relatively low, thus, the range to which the SOI timing can be delayed appears rather limited.

When the pilot injection amount is 5.8 mg, the misfire occurred due to the failure to establish a temperature and pressure environment sufficiently high to cause spray combustion of the main injection through pre-combustion in all the SOI timing regions. As for the remaining pilot injection conditions, it can be seen that the $IMEP_g$ graph in which the left side disappears in the V shape is drawn unlike the case where the total fuel amount is 23.1 mg and 34.6 mg. Due to the further increased amount of main injection, the SOI timing can hardly be advanced before the pre-combustion timing, and the region of the partially pre-mixed combustion shown in Fig 3. 3 disappears, resulting in the trend shown in Fig 3. 9.

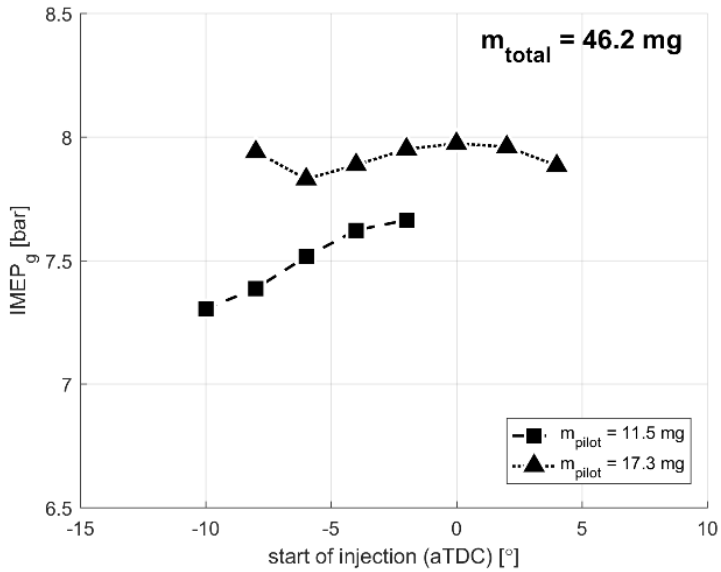

Figure 3. 9 $IMEP_g$ with varying SOI timing and ratio of pilot and main injection

Chapter 4. NO production analysis

4.1 Mechanism of NO production in ammonia spray

As explained in previous sections, since ammonia does not contain carbon in its molecular structure, it does not produce carbon-related emissions in the combustion process of ammonia, but it can produce various nitrogen-related emissions including NO, NO_2, and N_2O. This section focuses on NO, which accounts for the largest portion of the emissions which can be produced from the ammonia engines, and identifies the mechanism of production and analyzes the effect of various parameters on NO production.

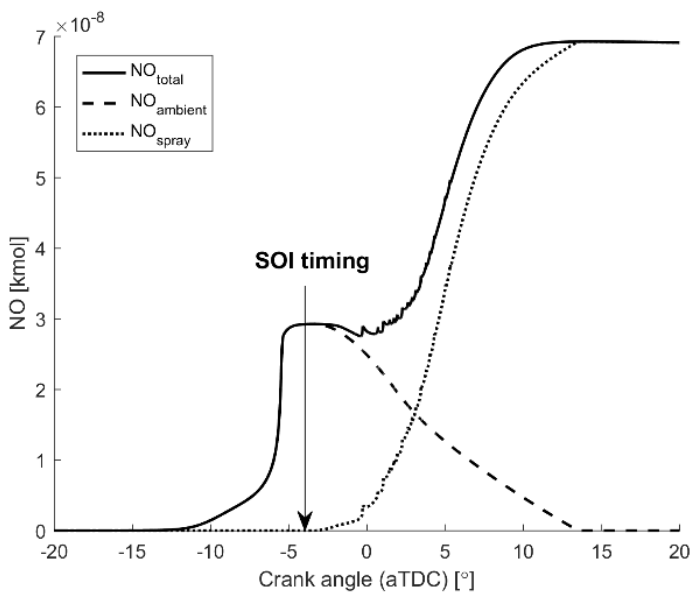

Figure 4. 1 NO profile inside the entire cylinder

Fig 4. 1 illustrates the total NO change in the cylinder under the simulated conditions of the pilot injection quantity of 11.5 mg, the main injection quantity of 23.1 mg and the SOI timing of -4 CAD aTDC. In the Fig 4. 1, the region where NO is generated is divided by the ambient zone ($NO_{ambient}$) where NO is produced through the pre-combustion and the spray zone (NO_{spray}) which is fuel region of main injection. As the piston approaches the TDC, the ammonia is oxidized by the high temperature and high pressure inside the cylinder, and at the same time, the NO gradually increases, and NO is abruptly increased with the pre-combustion near -6 CAD aTDC. Since then main spray of ammonia is injected at -4 CAD aTDC and NO in the ambient zone decreases relatively slowly due to the entrainment of the ambient into the spray zones. In this case, the ambient region is mainly composed of air, and the combustion products H_2O and N_2 generated by pre-combustion are included together with NO. In the spray area, the amount of NO is determined by the amount of NO entrained from ambient zone and NO produced by spray combustion. In the initial stage of main spray injection (-3 ~ 0 CAD aTDC), the NO_{spray} gradually increases in the spray zone, and the total NO_{total} in the cylinder decreases during the same period. Therefore, it can be seen that NO is actually consumed in that region. After that, the NO production in the spray zones becomes dominant rather than the NO consumption, and the NO_{total} increases. Since there is a limit to understanding the precise mechanism of NO production by merely checking the total NO change in the cylinder, the analysis of the specific fuel spray zone was performed.

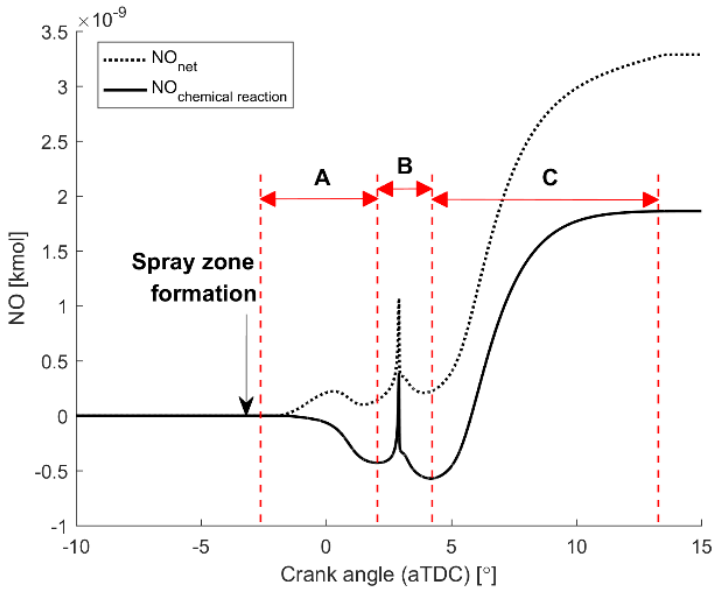

Figure 4. 2 Division of NO production process which occurs in a single spray zone

Fig 4. 2 represents NO changes in one spray zone under the simulation conditions shown in Fig 4. 1. As we have seen, NO change in the spray zone is affected by the NO from ambient zone as well as NO produced by ammonia oxidation. In order to analyze the production of NO from a perspective of chemical kinetics, the amount of NO generated through chemical reaction in the spray zone, excluding the NO inflow from the outside, is plotted by a solid line on the graph. The dotted line on the graph shows the amount of change in NO taking into account both the chemical reaction and the inflow from the ambient.

In this study, the process of NO production (or consumption) in the spray zone is divided into three phases A, B and C as shown in Fig 4. 2. The A, B, and C sections are referred to as Reduction NO phase, Combustion NO phase, and Thermal NO phase, respectively. It is possible to classify all the NO

production processes in various SOI timing and load operation conditions discussed in Section 3.2 above into three phases from a qualitative point of view though there is a difference in the absolute value of NO produced/consumed in each section.

A (Reduction NO phase) is a period from the point at which the product of pre-combustion and air begin to be entrained from the ambient zone to the point where the combustion starts. As the crank angle increases, NO decreases by chemical reaction. The boundary between the A and the B described later is the lowest point of the NO where the NO production reaction begins to dominate rather than the NO consumption reaction. In this phase, NO which is produced by the pre-combustion in the ambient zone and entrained into the spray zone is consumed by NH_2 produced from the ammonia in spray of main injection. Because of the relatively low temperature and oxygen concentration at the beginning of the spray formation, the consumption reaction prevails rather than the production of NO, resulting in a net decrease in NO. The NO reduction at this time is the same as that occurring in the Selective Non-Catalytic Reduction (SNCR) process, which reduces NO by using urea or NH3 as a reagent in the power plant.

B (Combustion NO phase) is a section where NO is produced and consumed as an intermediate product through the combustion of ammonia. The changes in NO occurring in this section can be understood by dividing into three steps again as shown in Fig 4. 3. In the first section, a sudden increase in NO occurs after combustion based on a sufficient amount of oxygen entrained into the spray zone during the ignition delay. The chemical reaction path of

ammonia at this time can be seen in Fig 4. 4. HNO is produced via NH_2, NH, and H_2NO, and the HNO produced undergoes reactions such as HNO + M ⇔ NO + H + M to produce NO. The produced NO is consumed by reacting with NH_i radicals (i = 0, 1 and 2. 0 means no hydrogen), which consumes less than the amount of NO produced from HNO, resulting in increased total NO.

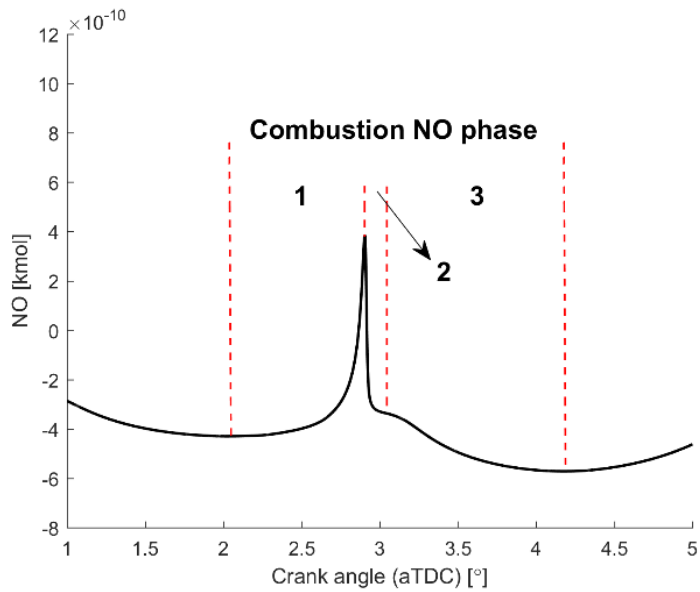

Figure 4. 3 Detailed classification of Combustion NO phase

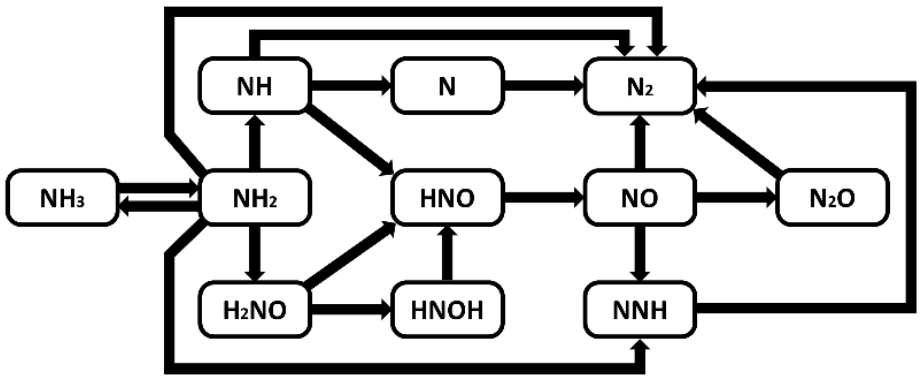

Figure 4. 4 Reaction pathway of ammonia oxidation

The second and third sections appear when combustion occurs under ammonia-rich conditions. In the second section combustion sustained through the oxygen entrainment from the ambient zone under very ammonia-rich conditions formed by consumption of oxygen through the combustion of first section and a continue of ammonia injection. Due to the rich condition, the production of NO through HNO is suppressed and the amount of NH_i radical is increased, thereby promoting the consumption of NO. As a result, rapid NO reduction occurs as shown in Fig 4. 3.

In the third section, NO is consumed under a condition where most of ammonia and NH_i radicals are consumed and only H_2 and H remain abundantly. Reverse reaction of HNO + M ⇔ NO + H + M, which contributed most of NO in the first section, occurs under lack of oxygen and rich H after combustion, resulting in NO reduction. Then, the oxygen become rich through continuous entrainment of oxygen from the ambient zone, H consumption increases, and NO consumption through HNO + M ⇔ NO + H + M stops. At similar times, the production of thermal NO via the extended Zeldovich

mechanism begins, based on the rich oxygen and the high temperature after combustion.

C (Thermal NO phase) in Fig 4. 2 is the period during which thermal NO is produced by continuous oxygen entrainment at high temperature after combustion. Backward reaction of $N_2 + O \Leftrightarrow NO + N$, which is one of the reaction of the extended Zeldovich mechanism, is dominant during combustion due to N produced from ammonia. As the oxygen is entrained after combustion, the forward reaction becomes dominant and $N_2 + O \Leftrightarrow NO + N$ makes the largest contribution to NO in the Thermal NO phase. The point where the forward reaction of N2 + O ⇔ NO + N becomes dominant is defined as the beginning point of Thermal NO phase. The amount of NO produced in this phase is mainly influenced by the temperature and oxygen concentration of the zone. In some cases, the NO concentration in the zone may also be affected.

4.2 Influence of SOI timing on each phase of NO production

To confirm the NO emission characteristics of the ammonia combustion strategy proposed in this study and to determine the optimal SOI timing in terms of NO emission, the simulation was carried out with the fixed total fuel amount of 34.6 mg, and the ratio of the pilot injection amount to the main injection amount of 1: 2 (11.5 mg : 23.1 mg).

The results obtained from the simulation are shown in Fig 4. 5. The bold black solid line on the graph is the total amount of NO produced in the

whole region inside the cylinder including ambient zone and fuel spray zones. The gray solid line (Pre-combustion NO phase) indicates NO produced as the lean mixture of pilot injected fuel and air is auto-ignited, which is obtained by considering NO production only in ambient zone. The rest of gray lines presents the NO productions of each phase in the spray of main injection. Total NO production is highest at the main injection timing -12 CAD aTDC, and decreased as the SOI timing is delayed.

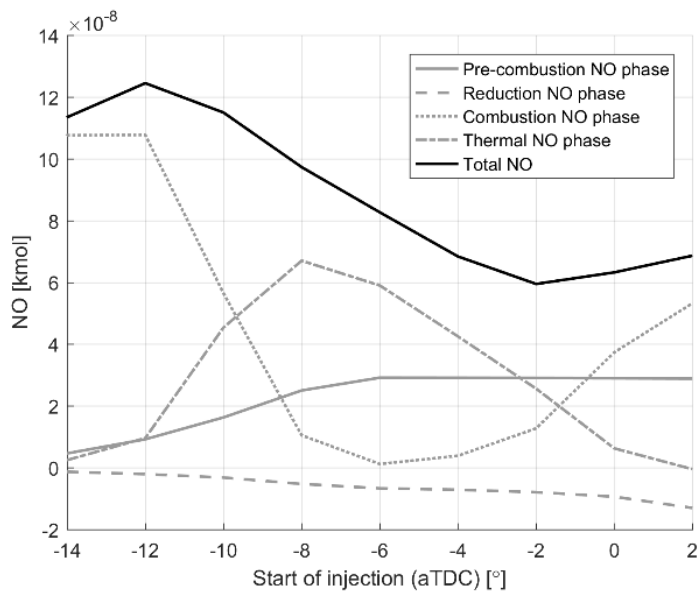

Figure 4. 5 NO productions in each phase of NO production under different SOI timing

This trend can be explained by analyzing NO production in each phase. First of all, the amount of NO production in the Pre-combustion NO phase increases until the SOI is -6 CAD aTDC, and thereafter it shows a constant value. These results are related to the pre-combustion timing under no

influence of the main injection. Fig 4. 6 shows the pressure profile of the cases with SOI timing of -14 and 0 CAD aTDC and the case with pilot injection only. If there is only the pilot injection or the main injection timing is delayed after TDC, the pre-combustion will occur at about -6 CAD aTDC. For the case with the earlier SOI timing the main spray, the pre-combustion will be delayed as shown in Fig 4. 6. With early SOI timing, the charge cooling of the main injection causes the temperature to drop and the pre-combustion to be delayed. At same time, the extent of the pre-combustion decreases due to entrainment of lean ammonia-air mixture to be used for the pre-combustion into the spray zones. As the SOI timing increases, the amount of lean ammonia-air mixture being entrained into the spray zone increases and consequently the amount of NO produced by pre-combustion in the ambient zone is reduced. A portion of the lean ammonia-air mixture entering the spray zone due to the advanced SOI timing may also contribute to NO production in the Combustion NO phase by being combusted with the ammonia of main injection.

In the Reduction NO phase, NO reduction increases (more negative) as the SOI is retarded. This can be explained by the NO production in Pre-combustion NO phase and the variation of spray mixing time with different SOI timing. The spray mixing time referred to here is the elapsed time from the SOI to the CA50 for the main injection. It can be seen that the spray mixing time according to SOI timing in Fig 4. 7 shows the minimum value at -6 CAD aTDC and increases with distance from –6 CAD aTDC. As the spray mixing time increases, the entrainment of ambient zone into the spray zones increases and the amount of NO to be reduced increases. Thus, it can be expected that

the lowest NO reduction is achieved at -6 CAD aTDC with the shortest spray mixing time. However, as SOI is advanced further, the amount of NO production in the Pre-combustion NO phase decreases due to the decrease in the extent of the pre-combustion, which leads to the decrease of NO reduction for the advanced SOI timing as shown in Fig 4. 5.

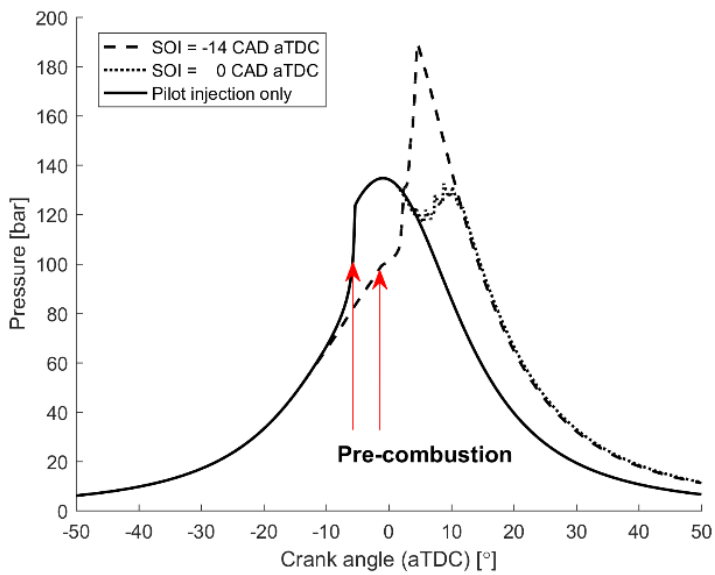

Figure 4. 6 Change in the timing of pre-combustion with different SOI timing and without main injection

NO production in Combustion NO phase has a minimum value when SOI is near -7 to -5 CAD aTDC and NO production is increased as the SOI timing is advanced or retarded around this point. This trend can also be explained mainly by the variation of spray mixing time according to SOI timing in Fig 4. 7. As the spray mixing time increases, the equivalence ratio at

the start of combustion is lowered, which results in the net increase of NO through the increase of NO production in first section and the decrease of NO reduction in second section on Fig 4. 3. Therefore, the NO change trend in the Combustion NO phase is similar to the trend of spray mixing time.

The additional discussion on the trend of the spray mixing time, which has a great effect on the Reduction NO phase and the Combustion NO phase, is as follows. In order for the ignition of the main injected fuel to occur rapidly after the injection point, that is, to shorten the spray mixing time, active mixing of the spray should occur near the TDC where the high temperature and high pressure are maintained by geometric compression and pre-combustion. At same time, main spray of ammonia should not be injected too early not to interfere with pre-combustion, as shown in Fig 4. 6. Under the given conditions, the maximum temperature of the ambient zone appears immediately after pre-combustion, closer to the pre-combustion than the TDC due to the heat transfer effect. As a result, the spray mixing time is the shortest when main spray of ammonia is injected at -6 CAD aTDC by the influence of the peak temperature occurrence time and the time required for initial spray formation and mixing. In this case, the increase in mixing time is greater when the SOI timing is advanced before -6 CAD aTDC than the case of SOI timing retarded after -6 CAD aTDC. This is due to injection at an earlier timing, which interferes with pre-combustion, delaying pre-combustion timing and decreasing the temperature by pre-combustion.

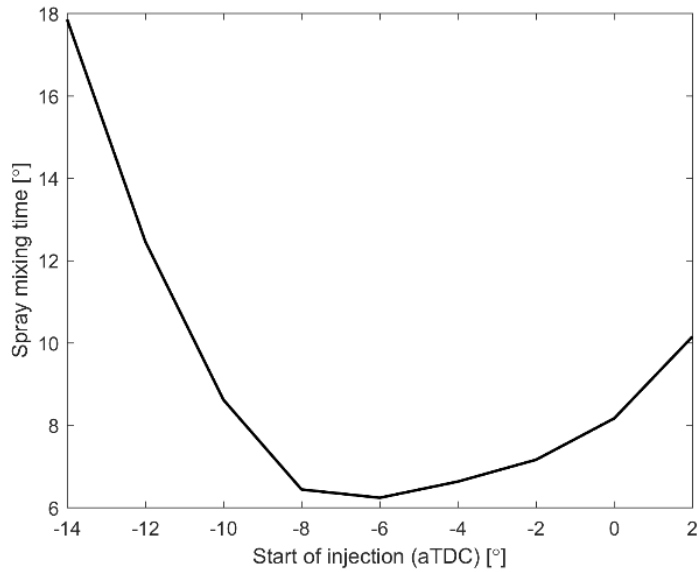

Figure 4. 7 Spray mixing time at different SOI timing

NO production in the Thermal NO phase is contrast to the Combustion NO phase. In this phase, the largest amount of NO is produced when the SOI timing is near -8 CAD, and the NO production amount decreases as the distance from this point increases. As is commonly known, the main factor influencing thermal NO production is temperature. Fig 4. 8 represents the change in NO in the Thermal NO phase versus the peak temperature of each fuel spray area for various SOI timing, which shows relationship of the peak temperature and the NO production in the Thermal NO phase. However, for the SOI timing is earlier than -10 CAD aTDC, the distribution of net NO change is somewhat deviated from the trend. The reason for this can be explained by the graph on Fig 4. 9.

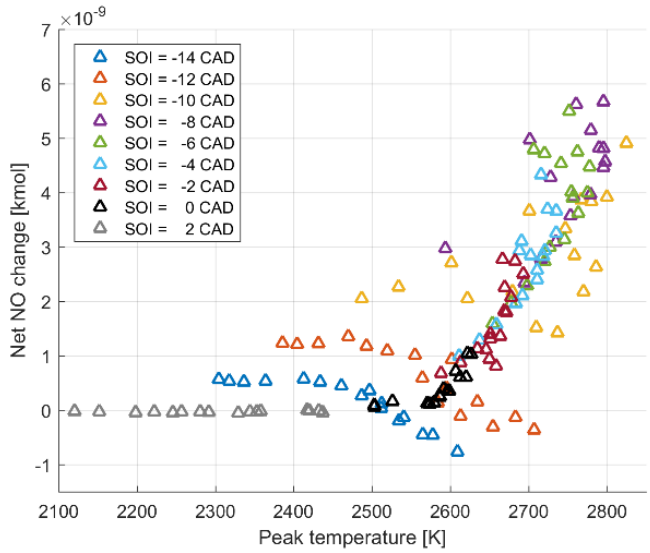

Figure 4. 8 Relationship between Net NO change in Thermal NO phase and the peak temperature of each spray zone

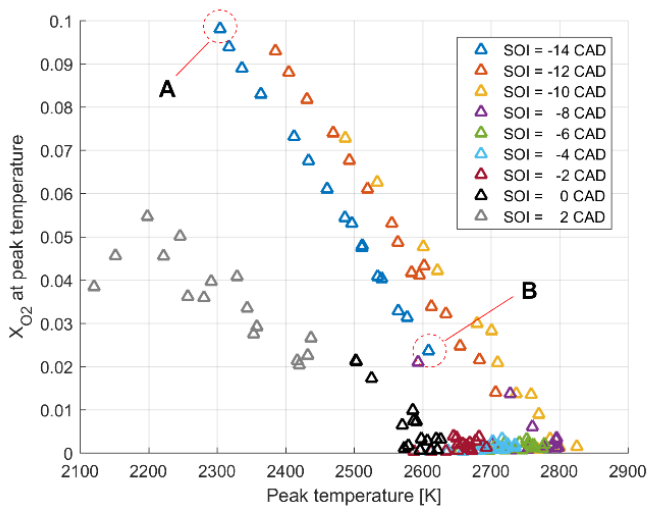

Figure 4. 9 Peak temperature and the mole fraction of oxygen at the point of peak temperature

As shown in Fig 4. 9, it can be seen that the points corresponding to the early SOI timing (before -10 CAD aTDC) showing the scattered distribution in Fig 4. 8 are high in the O_2 mole fraction at the peak temperature point, which means that the lean combustion occurred. This is caused by a large amount of entrainment from ambient zone into the spray zone before combustion due to the increase of the mixing time described above in Fig 4. 7. For the cases with the SOI timing at -8 CAD aTDC or later, where the spray mixing time is relatively short, combustion starts at an equivalence ratio of 1 or more, and a low O_2 mole fraction of less than 0.5% is observed at a peak temperature point. The amount of O_2 after the peak temperature point is determined by the entrainment from ambient zone. In the given condition, the entrainment rate from ambient of the most outer spray zone and the most inner fuel spray zone is about twice as much, thus, the O_2 mole fraction of each fuel spray zone is up to twice the difference. This difference in the amount of O_2 increases the thermal NO by up to 2 times in the fuel spray zones at the same peak temperature, however, it is not enough to disturb the trends in the relationship between peak temperature and thermal NO in Fig 4. 8. Additional analysis of two cases with extreme O_2 mole fractions at the SOI timing -14 CAD aTDC was carried out in order to understand the trend of NO formation at the SOI timing condition where the amount of O_2 mole fraction is relatively high at the peak temperature point due to a large amount of the entrainment from ambient zone.

Fig 4. 10-(a) and (b) show NO changes according to the crank angle in the A and B spray zone shown in Fig 4. 9, respectively. The amount of NO

in the equilibrium state (hereinafter referred to as NO_{eq}) of each crank angle is indicated by a dotted line on the graph. Under the given SOI timing of -14 CAD aTDC, lean combustion occurs in all spray zones, but there is a difference depending on the physical location on the spray. “A” is the zone located at the most outer in the spray, which starts to burn in a very lean condition, and even after all fuel is consumed, a molar ratio of about 10 % of oxygen remains. Due to the abundant amount of oxygen, NO_{eq} is high enough even though the peak temperature of the A spay zone is as low as 2300 K, which is lower than that of other spray zones, and thermal NO is produced as a result.

B is the zone located in the most inner of the spray. The NO_{eq} of B spray zone is relatively low due to the small amount of oxygen compared with A spray zone, and NO production in the Combustion NO phase is as high as NO_{eq} due to lean burn. NO_{eq} is decreased along with the temperature drop during the expansion process, and NO in the cylinder is also decreased accordingly. The reaction freezes soon after that.

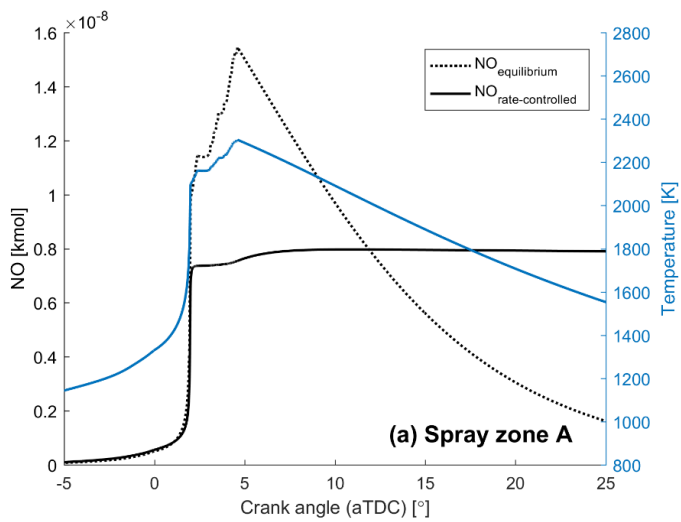

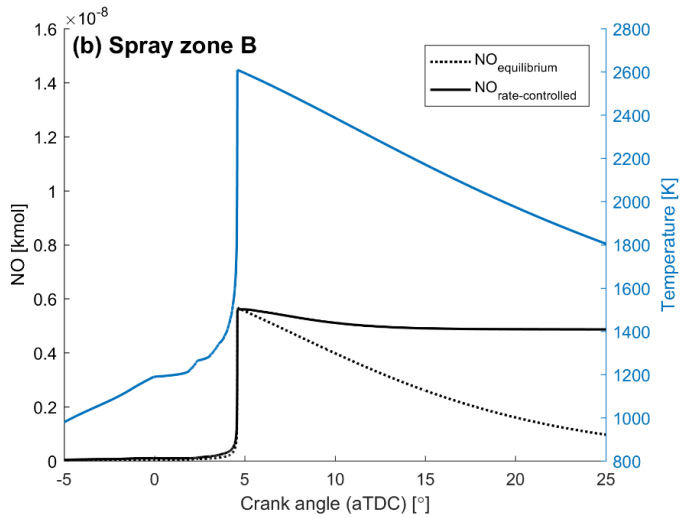

Figure 4. 10 Comparison of NO quantity and the amount of NO at equilibrium condition of two zones under extreme condition

As a result, when the combustion starts at a lean condition with an equivalence ratio of 1 or less, a large amount of NO is produced through the Combustion NO phase in common, and there is not a large difference in production amount depending on the lean degree. There is, however, a large difference in the value of NO_{eq} according to the equivalence ratio at the start of combustion. Therefore, as the equivalence ratio at the beginning of the lean burn is very low, that is, as it is located at the outer part of the spray, thermal NO is produced because the NO_{eq} is high enough even though the temperature is low and a large amount of NO is already produced through the Combustion NO phase. As spray zone is located at the inner part of the spray, NO_{eq} is as low as or lower than the amount of NO inside the spray zone due to relatively small amount of oxygen after the combustion, which results in the small amount of NO production or even reduction of NO through the Thermal NO

phase

The NO production trends in Fig 4. 5 are summarized as follows. The NO production at the earliest SOI timing condition is mostly originated from the Combustion NO phase, ie, fuel ammonia of spray combustion, and decreases as the SOI timing is delayed. At the same time, as the SOI timing is retarded, the NO production in the Thermal NO phase increases because the combustion timing approaches TDC and the temperature throughout the spray zones rises. However, total NO production is decreased because the amount of NO production in the Combustion NO phase is larger than the amount of NO production in the Thermal NO phase. As the SOI timing is further delayed, the combustion timing is retarded and the NO production of the Combustion NO phase is increased again due to lean spray combustion. The increase amount at this time is relatively small due to the delayed combustion during the expansion. The NO production amount in the Thermal NO phase, at the same time, is decreased due to low combustion temperature by the timing delayed, therefore, the total amount of NO production is reduced.

4.3 NO production under varying amount of fuel used

4.3.1 Amount of main injection variation

In order to investigate the variation of the NO production according to the change of the main injection quantity, simulation was carried out for the case where only the main injection quantity was changed to 0.5 (11.5 mg) and 1.5 times (23.1 mg) from the simulation condition performed in section 3.4. The amount of pilot injection is fixed at 11.5 mg. The results are shown in Fig 4. 11. When the absolute amount of produced NO (Fig 4. 11-(a)) is compared, the least amount of NO is produced for all SOI timing with the main injection of 11.5 mg. The NO production trend for the SOI timing is similar in all three main injection conditions only with the difference of the operable SOI range. Since the amount of fuel used in all three conditions is different, the normalized value of produced NO to NH_3 has been compared in order to analyze them under equal conditions and the result is shown in Fig 4. 11-(b). The NO production relative to NH_3 is lowest in the condition with the main injection of 34.6 mg. To analyze the cause of this, the NO production of each phase was compared. The results are shown in Fig 4. 12-(a) ~ (d).

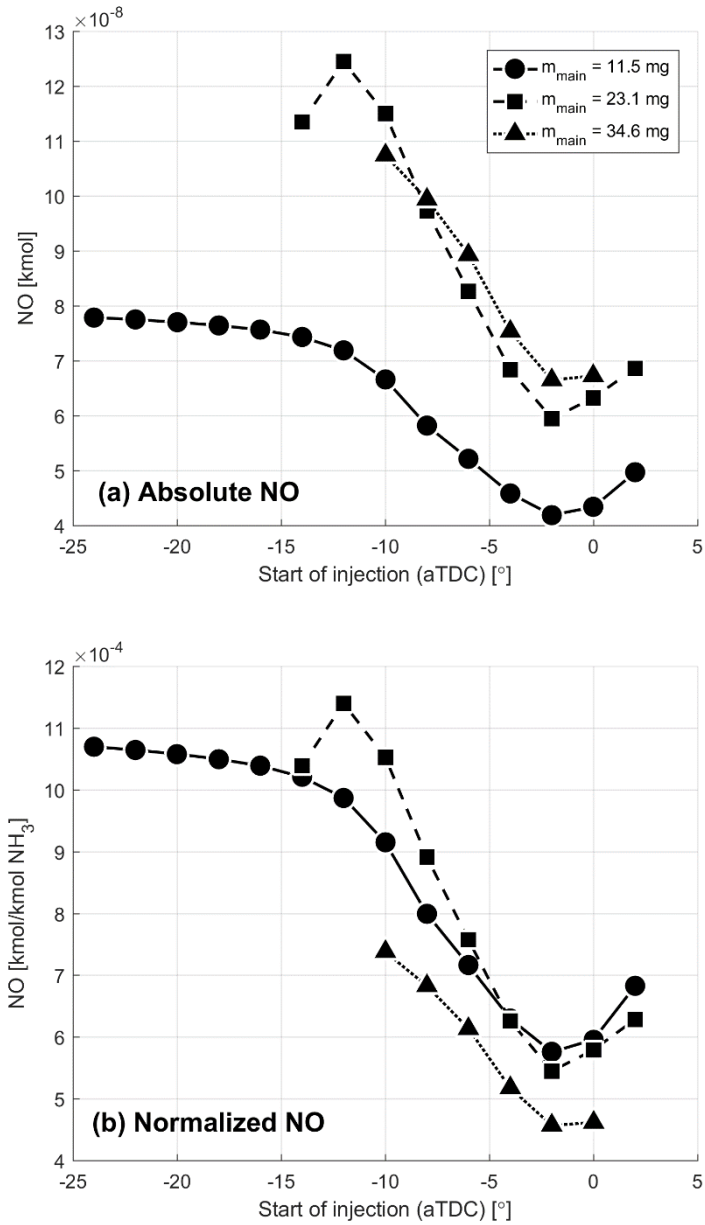

Figure 4. 11 NO production change (a) in absolute value and (b) in normalized value with variation of SOI timing and amount of main injection

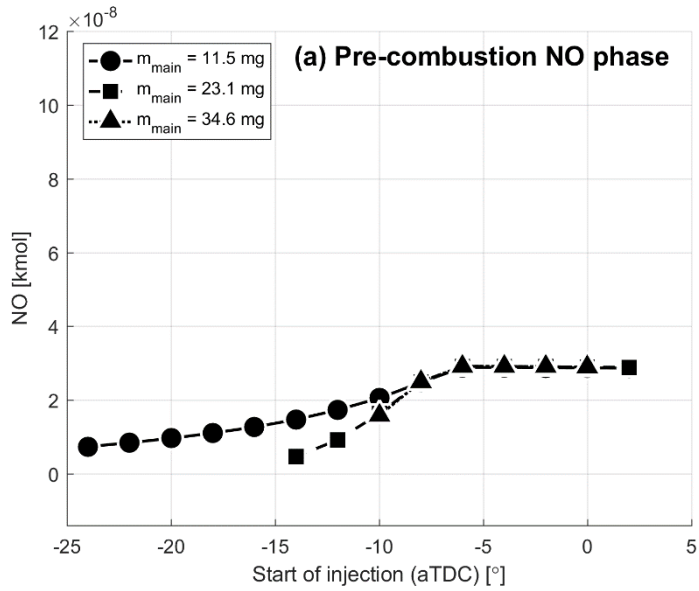
×10^-8
12
10
8
6
4
2
0
NO [kmol]
m_main = 11.5 mg
m_main = 23.1 mg
m_main = 34.6 mg
(a) Pre-combustion NO phase
-25
-20
-15
-10
-5
0
5
Start of injection (aTDC) [°]

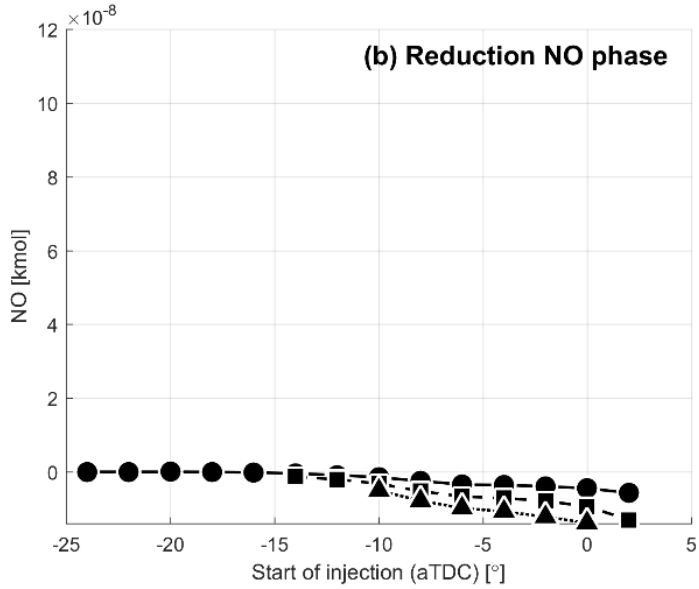
×10^-8
12
10
8
6
4
2
0
NO [kmol]
(b) Reduction NO phase
-25
-20
-15
-10
-5
0
5
Start of injection (aTDC) [°]

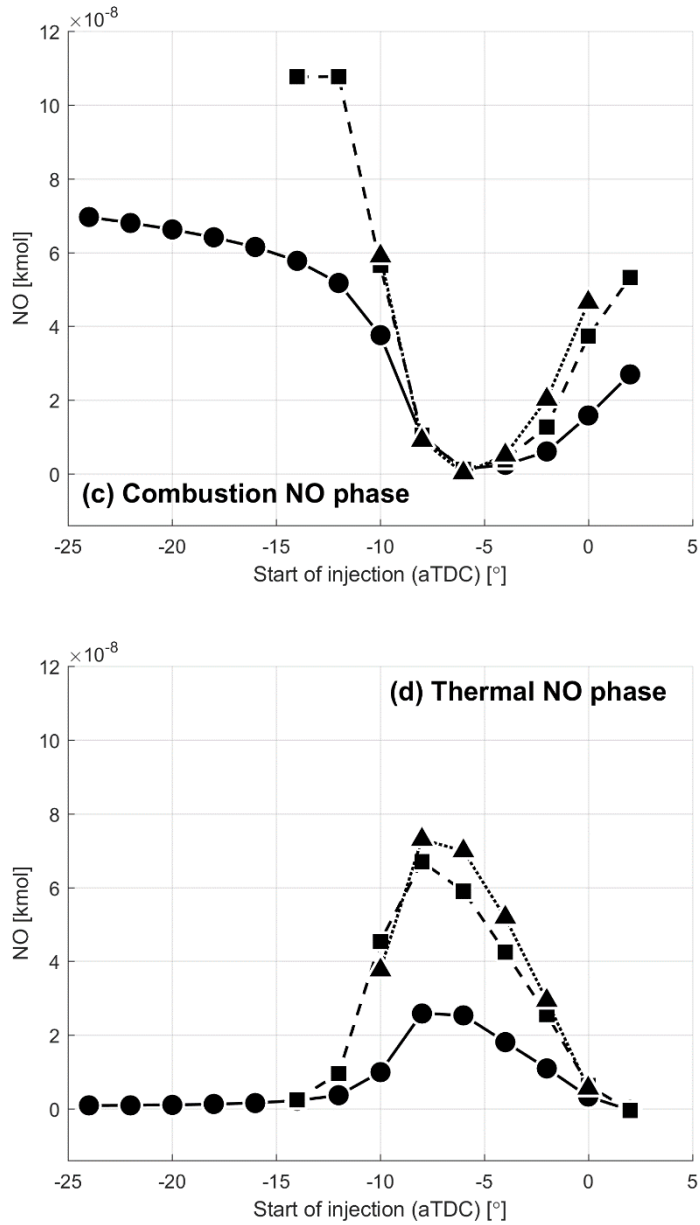

Figure 4. 12 NO production/consumption in each phase of NO production under different SOI timing and quantity of main injection

In all three cases, since the pilot injection quantity is constant, the same amount of NO is produced during the Pre-combustion NO phase for the

SOI timing after -6 CAD aTDC, the point at which pre-combustion occurs when there is no main injection. For earlier SOI timing, the amount of lean ammonia-air mixture entrained into spray zone increases as the SOI timing is advanced, leading to a reduction in the amount of mixture that can produce NO through the pre-combustion, therefore, NO production in the Pre-combustion NO phase is reduced. Also, if the main injection amount is increased for the same SOI timing, the injection period becomes longer and the amount of lean ammonia-air mixture entrained into the spray zone increases, so that NO in the Pre-combustion NO phase is decreased.

In the Reduction NO phase, the amount of NO reduction decreases in proportion to the main injection amount. This is due to the duration increased with the amount of main injection, which leads to the increased amount of entrainment from the ambient zone into the spray zone, so that NO to be reduced in the Reduction NO phase increases.

The following is a comparison of the Combustion NO phase. When the SOI timing is around -6 CAD aTDC, the ignition delay or spray mixing time is the shortest since the spray mixing occurs between the pre-combustion timing and the TDC and the temperature after pre-combustion is high enough cause very rich spray combustion. For this reason, in the Combustion NO phase, almost no NO is produced near the SOI timing of -6 CAD aTDC regardless of the main injection amount.

One noteworthy point is that NO production is similar in the Combustion NO phase at 23.1 mg of main injection and at 34.6 mg of main injection. To understand this, Fig 4. 13-(a) and (c) show the equivalence ratios

at the start of combustion in each spray zone when SOI timing is -10 CAD aTDC under three main injection conditions. Smaller axial index of spray zone shown in Fig 4. 13 means that the spray zone is formed earlier and located in downstream more. Larger radial index of spray zone represents that the spray zone is placed more near peripheral. For all cases, the equivalent ratios at the start of combustion in the spray zones whose axial indices are 1 and 2 (see Fig 2. 3 for indexing) are similar, however, in spray zones with higher axial index, there occurs richer spray combustion as the amount of main injection increases due larger amount and longer duration of main injection. In the spray zones formed early, NO is produced in proportion to the main injection amount because the equivalence ratio is not significantly different. In the spray zones of the axial index 4 which is formed at the latest stage, spray combustion occurs at a significantly rich condition and a relatively small amount of NO is produced in the condition with the main injection of 34.6 mg compared to the cases of main injection of 23.1 mg. As a result, considering the whole spray zone, NO productions in the Combustion NO phase of two conditions with the main injection of 23.1 mg and 34.6 mg are similar, but NO production in the Combustion NO phase with the main injection of 11.5 mg is slightly lower than those due to small amount of fuel used in main injection. Although not shown here, the NO production of the Combustion NO phase of the two conditions is similar for other SOI timing for similar reasons.

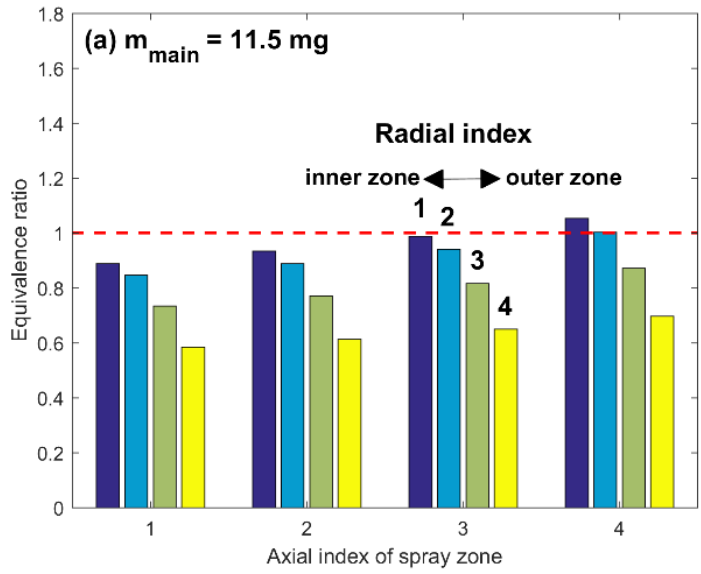
(a) m main = 11.5 mg
Radial index
inner zone
outer zone
1
2
3
4
Equivalence ratio
Axial index of spray zone
0
0.2
0.4
0.6
0.8
1
1.2
1.4
1.6
1.8
1
2
3
4

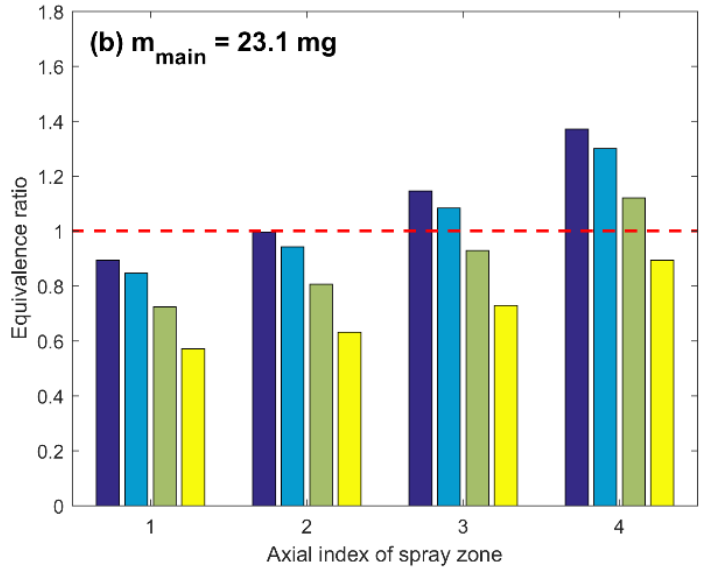
(b) m main = 23.1 mg
Equivalence ratio
Axial index of spray zone
0
0.2
0.4
0.6
0.8
1
1.2
1.4
1.6
1.8
1
2
3
4

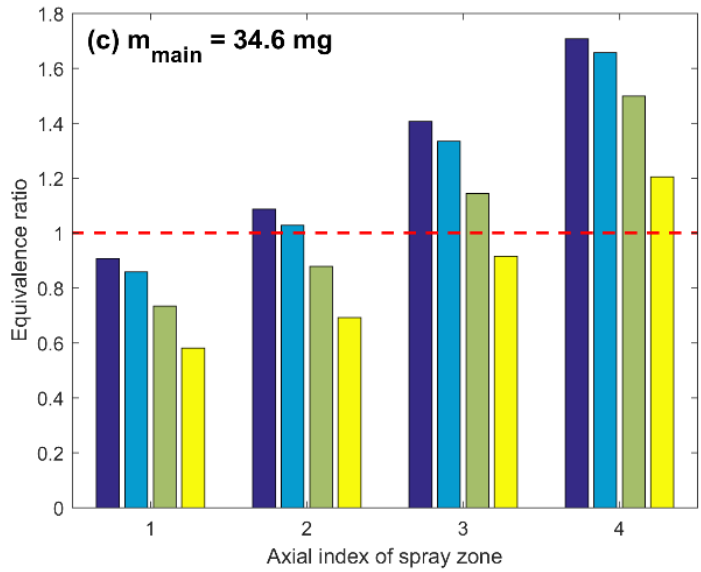

Figure 4. 13 Equivalence ratio of each spray zone at the start of combustion with different main injection condition

The NO production in the Thermal NO phase is the lowest at the main injection of 11.5 mg because the overall temperature rise is small due to the small amount of fuel used and the entrainment from the ambient zone into spray zone is limited by small volume of spray zones due to little fuel used, which causes the lack of oxygen needed to produce thermal NO. The NO production is similar in the rest of cases as in the Combustion NO phase. The cause of that can be explained through Fig 4. 14. The spray index shown in the Fig 4. 14 is the same as in Fig 4. 13. When the amount of main injection is 34.6 mg, in the spray zone of the axial index 1, the NO production is clearly higher than the case with the main injection of 23.1 mg. However, as the axial index increases, that is, as position of a spray zone approaches to upstream, the oxygen in the ambient zone become hard to be entrained into inner spray zones

due to the relatively larger injection quantity, resulting in a lack of oxygen required to produce the thermal NO, then, smaller amount of NO is produced compared to the case with main injection of 23.1 mg. Therefore, the amount of NO produced in the Thermal NO phase of the entire spray zone is similar, and it can be seen that a small amount of NO is produced compared to the amount of fuel used.

In summary, when the main injection amount is equal to or more than 34.6 mg, which is the amount of ammonia corresponding to the equivalence ratio of 0.6, the NO production through the Combustion NO phase and the Thermal NO phase in the spray zone is suppressed, resulting that the NO production amount compared to the ammonia used is rather lowered.

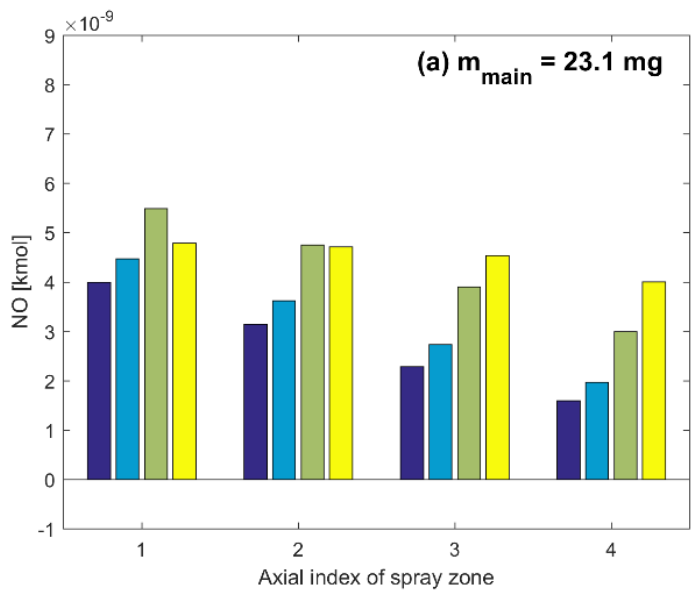

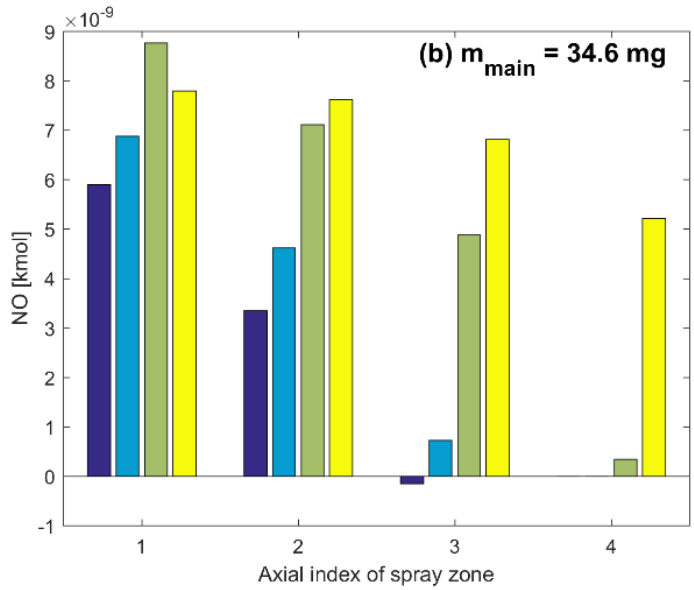

Figure 4. 14 Comparsion Thermal NO of each spray zone in two cases whose total values are nearly same

4.3.2 Amount of pilot injection variation

Next, the change in NO production amount was confirmed by changing the pilot injection quantity (5.8 mg, 11.5 mg, 17.3 mg) with fixed main injection amount of 23.1 mg, and the results are as shown in Fig 4. 15. The trend in Fig 4. 15-(b), where the NO is normalized with the amount of fuel used, is similar to the NO change trend (u-shape) according to SOI timing which was previously discussed, except for the case with the pilot injection of 5.8 mg. As the pilot injection quantity increases, the minimum value of the NO production amount relative to the fuel used tends to decrease. It can be seen

that the minimum NO production point appears on the later SOI timing, following the pre-combustion timing, as the amount of pilot injection increases

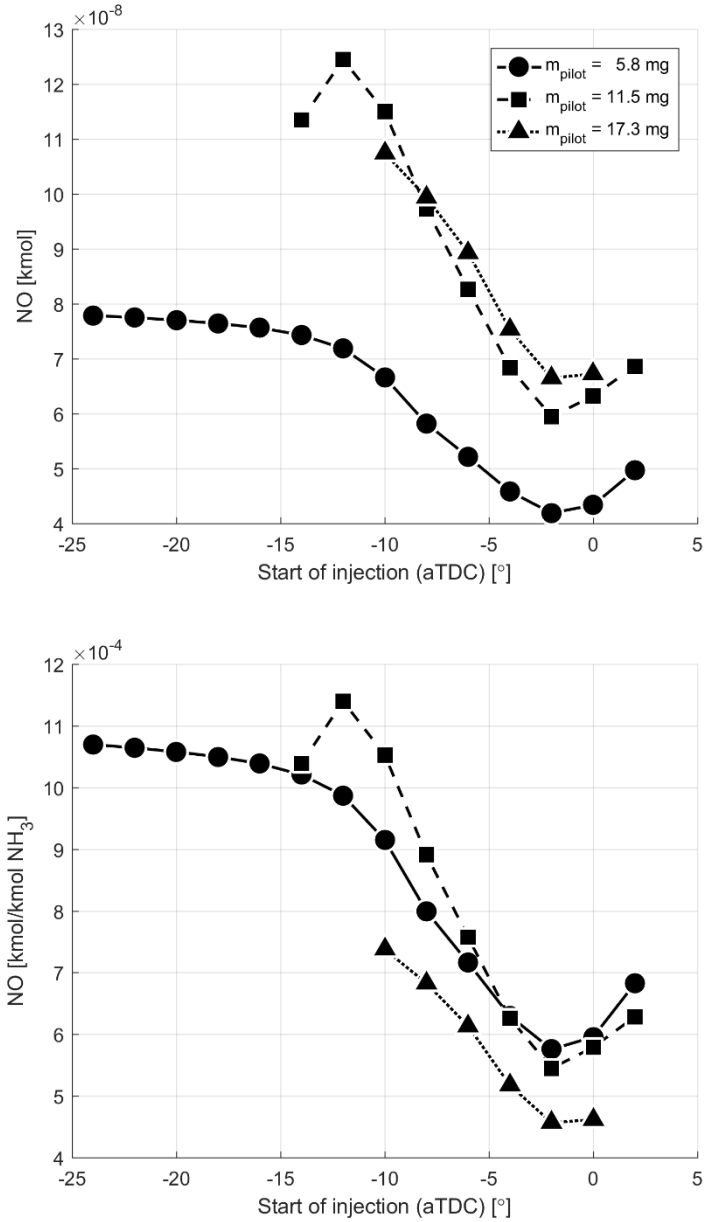

Figure 4. 15 NO production (a) in absolute value and (b) in normalized value under different SOI timing and amount of pilot injection

Fig 4. 16-(a) ~ (d) represents the NO production of each phase. In the Pre-combustion NO phase, as the pilot injection quantity increases, the timing where the NO is saturated is delayed due to delayed pre-combustion timing as illustrated on Fig 4. 16-(a). The point at which the NO production in the pre-combustion NO phase becomes zero, which means the misfire of the pre-combustion due to the early SOI timing, is also advanced as the amount of pilot injection decreases. The difference in NO reduction according to the amount of pilot injection shown in Fig 4. 16-(b) is caused by the difference in NO produced through the pre-combustion.

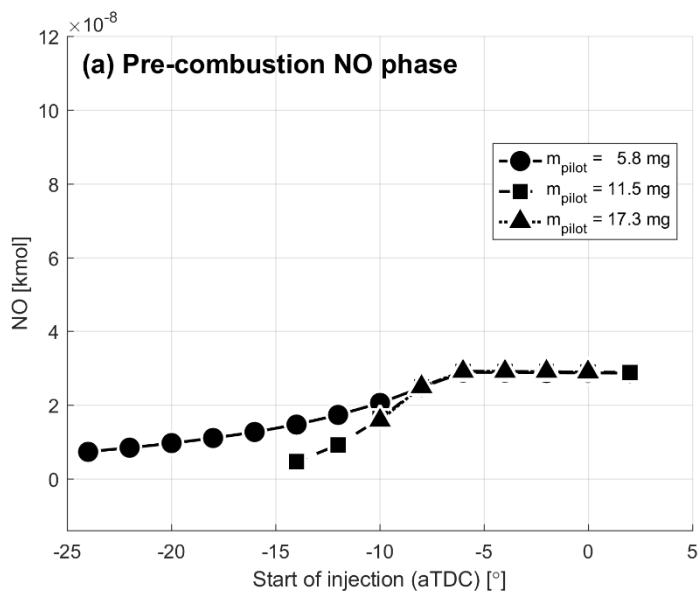

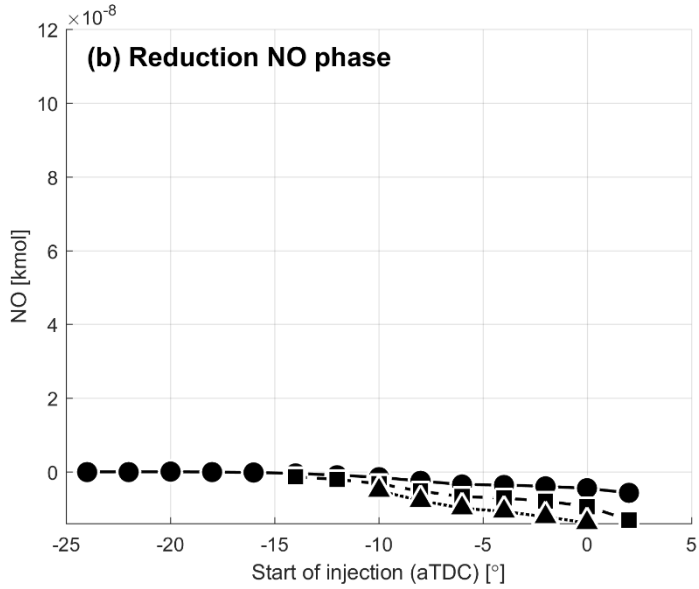
×10^-8
12
10
8
6
4
2
0
(b) Reduction NO phase
NO [kmol]
-25
-20
-15
-10
-5
0
5
Start of injection (aTDC) [°]

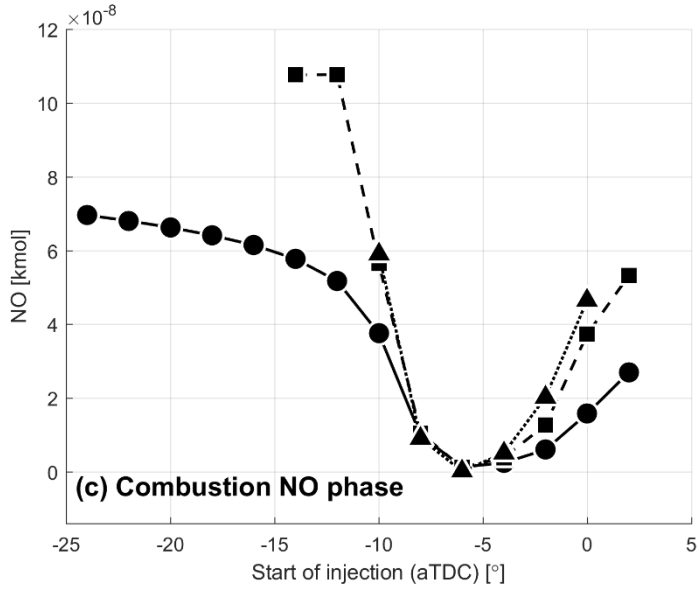
×10^-8
12
10
8
6
4
2
0
NO [kmol]
(c) Combustion NO phase
-25
-20
-15
-10
-5
0
5
Start of injection (aTDC) [°]

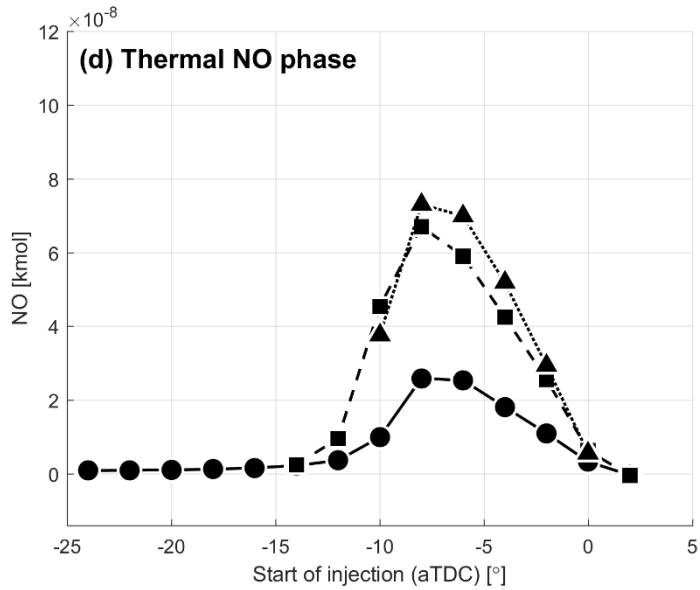

Figure 4. 16 NO production/consumption in each phase of NO production with varying SOI timing and quantity of pilot injection

In the Combustion NO phase, only the case with the pilot injection quantity of 5.8 mg has a different graph shape, which is a result of insufficient temperature and pressure rise through the pre-combustion. The pre-combustion did not raise temperature and pressure high enough to occur spray combustion of ammonia, resulting in lean spray combustion with longer mixing time for the whole range of SOI timing, therefore, downwardly deep convex shape, which is caused by rich spray combustion and can be found in the Combustion NO phase graph of other pilot injection conditions, does not appear. In addition, when the SOI is excessively advanced or retarded, the ignition delay is prolonged, resulting in the excessively lean spray combustion and the temperature after the spray combustion is lowered. The amount of NO

production is reduced due to temperature lowered, so that the both ends of the graph of the Combustion NO phase appear downward. In the case with the pilot injection amount of 17.3 mg, the pre-combustion timing is delayed but the temperature immediately after pre-combustion is higher than that of the case with pilot injection amount of 11.5 mg, so that the overall mixing time is reduced and the spray combustion starts at a richer condition. For this reason, the minimum value of NO production in Combustion NO phase decreases as the pilot injection quantity increases though the point where minimum NO appears is different.

Chapter 5. In-situ NO reduction

5.1 Additional stage of combustion strategy for NO reduction

Through Section 4, we examined the NO emission characteristics of the engine with the proposed ammonia combustion strategy. It was confirmed that NO emission in Combustion NO phase and Thermal NO phase can be suppressed and relatively small NO emission can be achieved by inducing rich spray combustion and delaying SOI timing as much as possible. However, even the lowest level of NO emissions has reached about 2900 ppm, so additional NO reduction method is required to actual utilization of the engine.

In this study, it is tried to reduce NO by using ammonia again as a reagent. Ammonia has been widely used as a reagent for selective non-catalytic reduction (SNCR) process to reduce NO produced in power plants. The SNCR process is a process in which NO is selectively reduced by a reagent containing amines (-NH-) or cyanides (-CN-) at a relatively high temperature of about 1000 °C. The SNCR reaction using ammonia as a reagent is described in Eq. (5. 1).

$$4NH_3 + 4NO + O_2 \leftrightarrow 4N_2 + 6H_2O \qquad (5.\ 1)$$

In the past, some attempts have been made to reduce NO by direct

injection of urea water or ammonia into the cylinder. However, the method used in the studies has disadvantages that in addition to the injector for fuel, an injector for urea or ammonia should be installed.

The NO reduction method to be applied in this study has a relative advantage over the previously studied methods since it is possible to utilize the injection system installed for the ammonia as fuel. In addition, since the high-pressure injection system used for fuel atomization can be also utilized as a system for the reagent injection, higher NO reduction rate can be expected.

5.2 Modification of spray model for in-situ NO reduction

In general, the amount of reagent used in the SNCR process is in the range of 3 times the molar amount of NO. This corresponds to 2.3 mg ammonia based on NO of 2900 ppm. The amount of ammonia to be used for in-situ NO reduction is much smaller than 11.5, 23.1, and 34.6 mg, which is the amount of ammonia used in the main injection in previous sections, so some modification of the model is required prior to performing the simulation.

The spray model used in this study is valid only when the injection duration is relatively long, including the steady state over a most period of the injection duration. For the post-injection of ammonia to be used for in-situ NO reduction, which has shorter duration than general spray injection which occurs in engine, it is difficult to expect accurate prediction performance with the spray model used for main injection. In order to more accurately model the

pilot injection with short injection duration, Thoma et al. modified the penetration of spray to be proportional to $\frac{1}{\sqrt{t}}$ instead of being proportion to $\frac{1}{t}$ in the existing model[44].

For the amount of post-injection used in the simulation, the duration is less than 1/4 of the main injection. Therefore, the simulation was performed by reducing the number of grids in axial direction to one from 4 grids in axial direction and radial direction of main injection. Fig 5. 1 shows the schematic of post-injection for in-situ NO reduction.

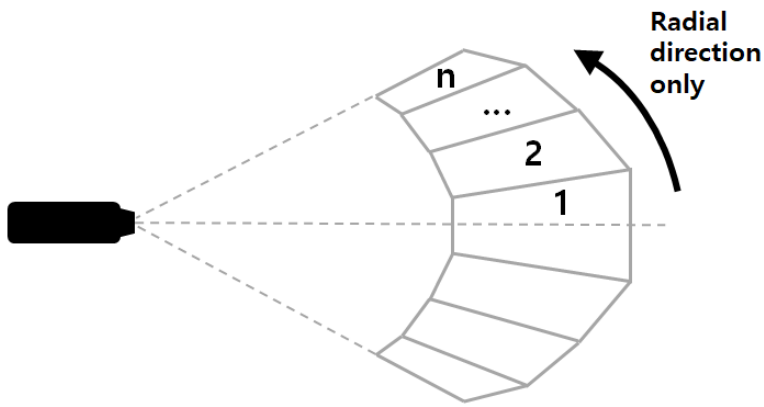

Figure 5. 1 Schematic diagram of spray model for post-injection

In this study, we modified the spray model for in-situ NO reduction and performed a parametric study on various ratios of NH_3, which is used as a reagent, to NO to be reduced and start of post-injection (SOPI) timing.

5.3 In-situ NO reduction under various start of post-injection timing

In this section, the effect of start-of-post-injection (SOPI) timing on NO reduction was verified and the cause the influence was analyzed. The temperature window at which the SNCR reaction is most active is between 1200 and 1400 K. In the simulations performed in the previous sections, the range of crank angles at which this temperature band appears is about 40 to 60 CAD aTDC. In this in-situ NO reduction, since the ammonia is not used in a pre-mixed state with product gas which contains the NO to be reduced, the effects of charge cooling and spray mixing time must be fully considered. In this study, in situ NO reduction was performed at 4 CAD intervals for SOPI timing in the range of 10 to 50 CAD so that sufficient mixing occurs until at least 60 CAD aTDC and NO reduction can occur.

Fig 5. 3 shows the NO reduction rate according to SOPI timing when the in-situ NO reduction with NH_3/NO of 3 was applied to the operating conditions under pilot injection of 17.3 mg, main injection of 23.1 mg and SOI timing of 2 CAD aTDC where NO of about 2900 ppm is emitted. In addition, the average temperature of cylinder at each SOPI timing is also shown in Fig 5. 3 to see the effect of the temperature on NO reduction rate. The NO reduction rate represents the highsest value for SOPI timing of 26 CAD aTDC, and the reduction rate changes sharply as the SOPI timing is advanced or delayed. The decreasing NO reduction rate for the retarded SOPI timing is to be due to the

temperature decrease occurring during the expansion process. In the range of crank angle 30 to 35 CAD aTDC, the temperature of the cylinder is about 1600 K, at which the SNCR reaction occurs actively. The temperature of the post-injected spray zones at the time of the actual reaction will be lower than this because the SNCR reaction may occur after sufficient mixing with ambient gas. For this reason, under SOPI timing conditions delayed than 30 CAD aTDC, NO reduction is less than 5%. On contrary to this, reduction of reduction rate due to advanced SOPI timing occurs from other causes. From the temperature profile shown in Fig 5. 3, it can be seen that the combustion of main spray injection is completed near 15 CAD aTDC, which suggests that the high temperature after combustion may have affected the decreased NO reduction rate.

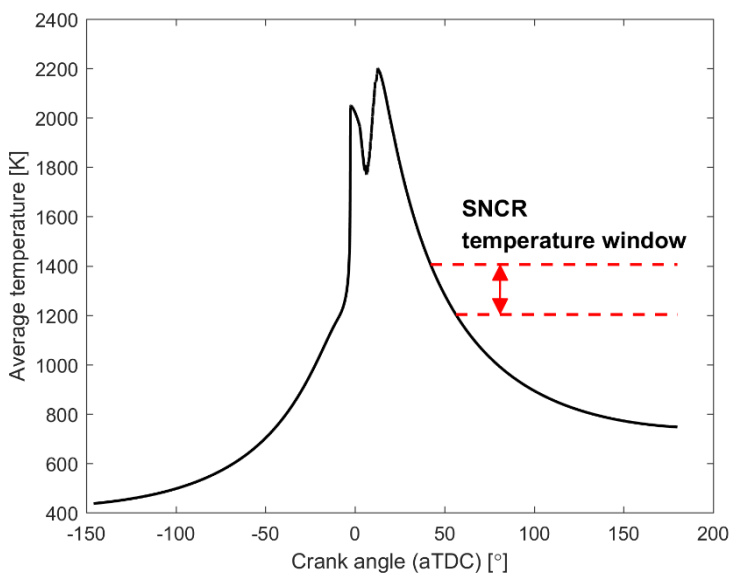

Figure 5. 2 SNCR temperature window on the ammonia engine cycle

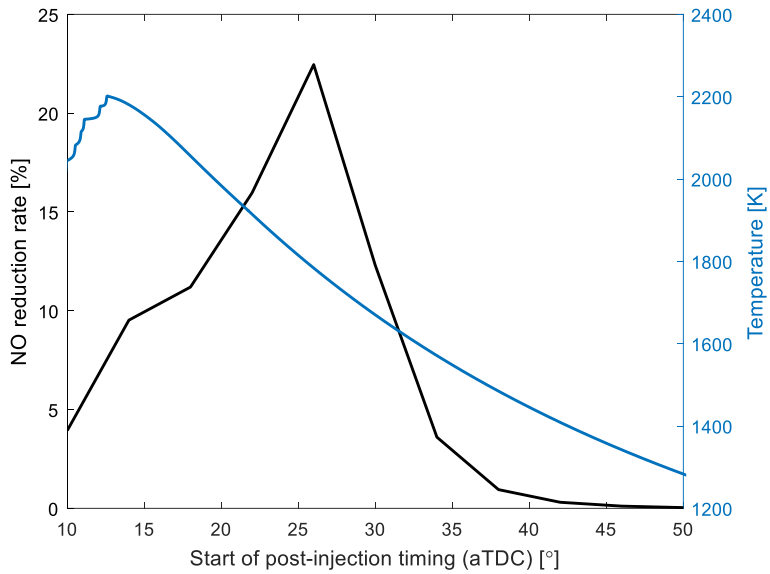

Figure 5. 3 NO reduction rate under different SOPI timing and temperature at the timing

Fig 5. 4 shows the temperature changes of each post-injected spray zone with varying crank angle under in-situ NO reduction conditions of SOPI timing of 10 CAD aTDC. The post-injected spray zone of radial index 4 is located at the outermost position of the spray, and since the entrainment of ambient gas is relatively large, the temperature rises the fastest, leading to combustion. In the remaining regions, it can be seen that the combustion is limited by the entrainment rate from ambient gas due to the influence of the relatively lower entrainment rate. In Fig 5. 5, the amount of NO present in each post-injected spray zone is indicated by the dotted line, and the amount of NO change due to the chemical reaction is indicated by a solid line. The radial index for each color is the same as in Fig. It can be seen that only the decrease

of NO occurs in whole crank angle range. This phenomenon can be analyzed in the same manner as in section 4. Under given conditions, combustion of the post-injected ammonia begins almost simultaneously with the entrainment of ambient gas without the Reduction NO phase, since the temperature inside the cylinder at the injection timing is sufficiently raised by the combustion of the main injection spray. The decrease in NO in the graph is the same as the decrease in NO in the late stage of the Combustion NO phase where NO is reduced under the lack of oxygen. The reduction of NO continues until ammonia is exhausted and thermal NO is not produced when the combustion NO phase ends unlike in the case of main spray injection, due to the reduced temperature through cylinder expansion.

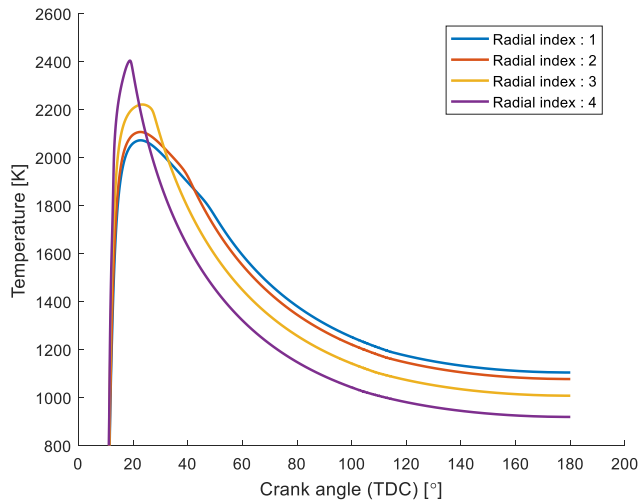

Figure 5. 4 Temperature profile of each post-injected spray zone at SOPI timing of 10 CAD aTDC

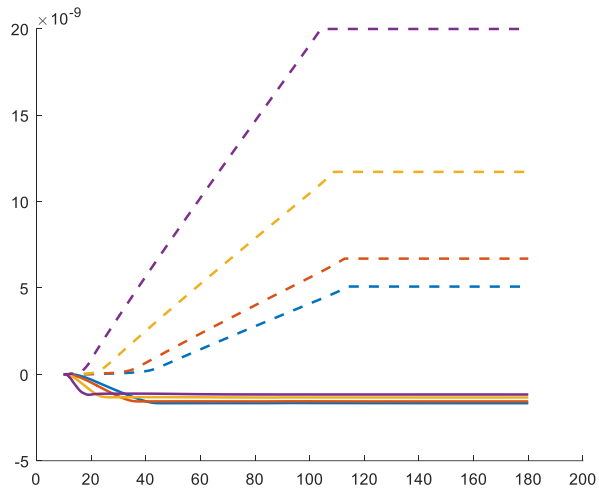

Figure 5. 5 NO in each post-injected spray zone (dashed line) and the NO change by chemical reaction (solid line) at SOPI timing of 10 CAD aTDC

Fig 5. 6 and 5. 7 represent in-situ NO reduction results under SOPI timing of 26 CAD aTDC conditions which is contrast to the result under SOPI timing of 10 CAD aTDC. SOPI timing of 26 CAD aTDC does not cause any further combustion even when the spray is sufficiently mixed with the ambient gas because the temperature of the cylinder has sufficiently decreased during the expansion process. The highest NO reduction rate could be obtained with the SOPI timing of 26 CAD aTDC since there no waste of ammonia through combustion and the SNCR temperature window was appropriately followed. However, ammonia slip, which is the emission of unreacted ammonia, may occur because the ammonia is not consumed through combustion, and the chemical reaction in the SNCR temperature window is relatively slow

compared to the combustion process. The ammonia slip under each SOPI timing condition is shown in Fig 5. 8. Results under SOPI timing of 26 CAD where the highest NO reduction rate appears shows a 7000 ppm ammonia slip which is 84 % of the amount of post-inject ammonia. This is because the NO reduction efficiency in the SNCR temperature window is relatively high, but the ammonia is not consumed because of the slow reaction rate due to the low temperature. Therefore, considering both NO reduction rate and ammonia slip, the most ideal SOPI timing can be concluded to be 22 CAD aTDC.

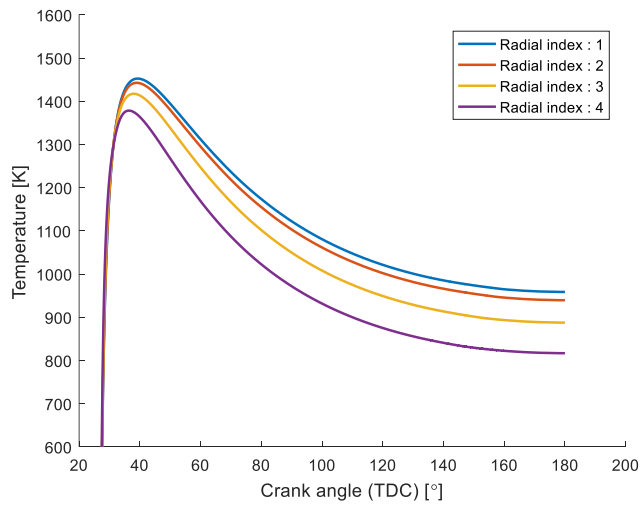

Figure 5. 6 Temperature profile of each spray zone of post-injection at SOPI timing of 26 CAD aTDC

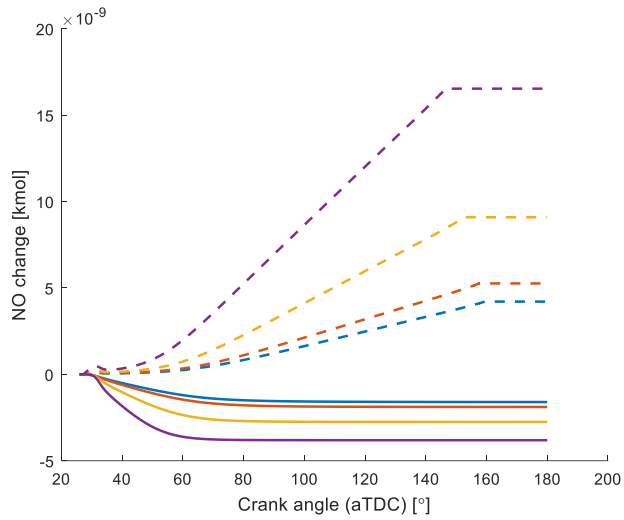

Figure 5. 7 NO in each post-injected spray zone (dashed line) and the NO change by chemical reaction (solid line) at SOPI timing of 26 CAD aTDC

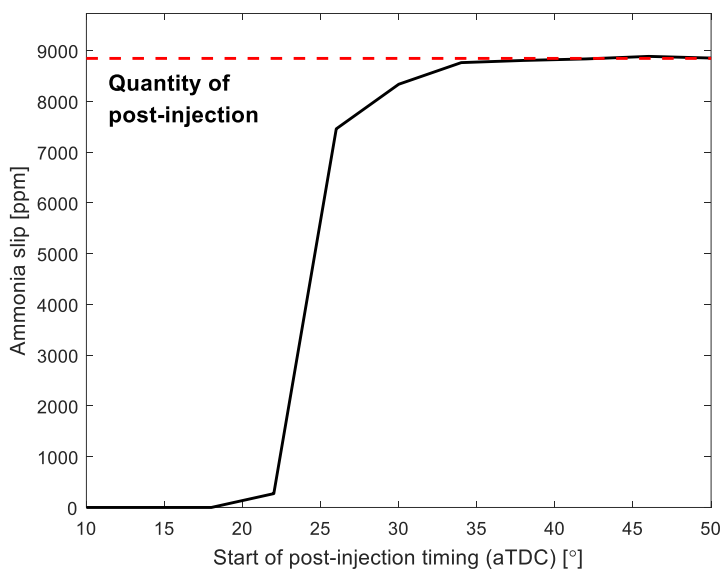

Figure 5. 8 Ammonia slip at different SOPI timing

Chapter 6. Conclusions

A new combustion strategy has been proposed for the use of ammonia in an internal combustion engine, and a parametric study has been conducted through simulations to confirm and analyze the operating characteristics of the engine with the combustion strategy. to validate the combustion strategy proposed, engine modeling was performed primarily. A detailed chemical reaction mechanism was used to more precisely predict the pre-combustion that is the auto-ignition of lean ammonia-air mixture, and NO production and consumption process, which are a characteristics of the proposed combustion strategy. In order to compensate the increased time cost by using the detailed chemical reaction mechanism, the quasi-dimensional model was selected and the engine was modeled to increase the prediction performance of the chemical reaction occurring inside the cylinder and to consider the physical characteristics of spray at same time.

At first, the simulation under various conditions with different the ratios of pilot injection to main injection and the SOI timing has been conducted for a fixed amount of total fuel used, and the basic characteristics of the proposed combustion strategy have been confirmed. As the pilot injection quantity increases, $IMEP_g$ tends to increase overall, and operable SOI timing expands owing to the increase in temperature after pre-combustion. When the pilot injection quantity is fixed, as the amount of total fuel increases, the amount of fuel used for the main injection also increases, such that charge

cooling is increased. Owing to the increased charge cooling, the pre-combustion may not occur as SOI is advanced too much. For this reason, the range of operable SOI timing becomes narrow with the increasing total fuel used. If the total fuel amount is increased to 46.2 mg, which corresponds to an equivalence ratio of 0.8 for a given engine geometry, the operable SOI range will be reduced to 8 CAD, and it will be difficult to operate the engine at a given compression ratio of 35:1 and intake temperature of 220 °C.

Next, the NO production process in the ammonia engine is divided into four sections, which are the pre-combustion NO phase, reduction NO phase, combustion NO phase, and thermal NO phase. The mechanism of NO production in ammonia engines was studied through the analysis of each phase. The pre-combustion NO phase is the period where NO is produced owing to auto-ignition of the lean ammonia–air mixture. The reduction NO phase is the period during which the NO entrained from the ambient zone is consumed in the rich spray zones at the initial stage of spray formation. The combustion NO phase is a period in which NO is produced through the spray combustion and is greatly influenced by the equivalence ratio at the start of combustion. Finally, the thermal NO phase is the section in which thermal NO is produced from the oxygen and nitrogen in air at high temperature after combustion. The amount of NO produced in the thermal NO phase is greatly affected by the temperature, and when the lean spray combustion of ammonia occurs, the amount of oxygen and the amount of NO weakly influence the NO from the thermal NO phase. As a result of the analysis of NO production in each phase, it was confirmed that when rich combustion occurs at slightly delayed SOI timing, NO

production in the combustion NO phase and thermal NO phase is inhibited, which leads to lowered net production of NO.

To reduce the NO produced in the ammonia engine which is as high as about 2900 ppm even in the condition where the smallest amount of NO is produced, SNCR process is added on the combustion strategy proposed, which has been called in-situ NO reduction in this study. Due to the injection system installed for the use of ammonia as an engine fuel, there is no need of additional installation of injection system for in-situ NO reduction.

The result of in-situ NO reduction shows that NO reduction of 25% can be achieved by injecting post-spray at 25 CAD aTDC. However, at the timing where the highest NO reduction rate appears, a considerable amount of ammonia is emitted without being fully reacted, therefore, SOPI timing should be adjusted minutely to avoid large amount of ammonia slip and to reduce NO efficiently.

Reference

[1] Energy R. Medium-Term Market Report 2014: Market Analysis and Forecasts to 2020 [online]. IEA.

[2] Mogi T, Kim D, Shiina H, Horiguchi S. Self-ignition and explosion during discharge of high-pressure hydrogen. Journal of Loss Prevention in the Process Industries. 2008;21:199-204.

[3] Reilly JJ, Sandrock GD. Hydrogen storage in metal hydrides. Scientific American. 1980;242:118-31.

[4] Sakintuna B, Lamari-Darkrim F, Hirscher M. Metal hydride materials for solid hydrogen storage: a review. International Journal of Hydrogen Energy. 2007;32:1121-40.

[5] Schüth F, Bogdanović B, Felderhoff M. Light metal hydrides and complex hydrides for hydrogen storage. Chemical communications. 2004:2249-58.

[6] Zheng J, Liu X, Xu P, Liu P, Zhao Y, Yang J. Development of high pressure gaseous hydrogen storage technologies. International Journal of Hydrogen Energy. 2012;37:1048-57.

[7] Lee S, Yi H, Kim E. Combustion characteristics of intake port injection type hydrogen fueled engine. International Journal of Hydrogen Energy. 1995;20:317-22.

[8] Karim GA. Hydrogen as a spark ignition engine fuel. International Journal of Hydrogen Energy. 2003;28:569-77.

[9] Heffel JW. NO x emission reduction in a hydrogen fueled internal combustion engine at 3000 rpm using exhaust gas recirculation. International Journal of

Hydrogen Energy. 2003;28:1285-92.
[10] Das L, Gulati R, Gupta PK. A comparative evaluation of the performance characteristics of a spark ignition engine using hydrogen and compressed natural gas as alternative fuels. International Journal of Hydrogen Energy. 2000;25:783-93.
[11] Akansu SO, Dulger Z, Kahraman N, Veziroğlu TN. Internal combustion engines fueled by natural gas—hydrogen mixtures. International journal of hydrogen energy. 2004;29:1527-39.
[12] Xing B, Savadogo O. Hydrogen/oxygen polymer electrolyte membrane fuel cells (PEMFCs) based on alkaline-doped polybenzimidazole (PBI). Electrochemistry communications. 2000;2:697-702.
[13] Corbo P, Migliardini F, Veneri O. Experimental analysis and management issues of a hydrogen fuel cell system for stationary and mobile application. Energy conversion and management. 2007;48:2365-74.
[14] Ahluwalia RK, Wang X. Direct hydrogen fuel cell systems for hybrid vehicles. Journal of Power Sources. 2005;139:152-64.
[15] Bartels JR. A feasibility study of implementing an ammonia economy: Iowa State University; 2008.
[16] Choudhary T, Sivadinarayana C, Goodman D. Catalytic ammonia decomposition: COx-free hydrogen production for fuel cell applications. Catalysis Letters. 2001;72:197-201.
[17] Metkemeijer R, Achard P. Comparison of ammonia and methanol applied indirectly in a hydrogen fuel cell. International journal of hydrogen energy. 1994;19:535-42.
[18] Yin S-F, Zhang Q-H, Xu B-Q, Zhu W-X, Ng C-F, Au C-T. Investigation on the catalysis of COx-free hydrogen generation from ammonia. Journal of Catalysis.

2004;224:384-96.

[19] Meng G, Jiang C, Ma J, Ma Q, Liu X. Comparative study on the performance of a SDC-based SOFC fueled by ammonia and hydrogen. Journal of Power Sources. 2007;173:189-93.

[20] Maffei N, Pelletier L, Charland J, McFarlan A. An intermediate temperature direct ammonia fuel cell using a proton conducting electrolyte. Journal of power sources. 2005;140:264-7.

[21] Xie K, Yan R, Chen X, Wang S, Jiang Y, Liu X, et al. A stable and easily sintering BaCeO3-based proton-conductive electrolyte. Journal of Alloys and Compounds. 2009;473:323-9.

[22] Westlye FR, Ivarsson A, Schramm J. Experimental investigation of nitrogen based emissions from an ammonia fueled SI-engine. Fuel. 2013;111:239-47.

[23] Ryu K, Zacharakis-Jutz GE, Kong S-C. Effects of gaseous ammonia direct injection on performance characteristics of a spark-ignition engine. Applied Energy. 2014;116:206-15.

[24] Ryu K, Zacharakis-Jutz GE, Kong S-C. Performance enhancement of ammonia-fueled engine by using dissociation catalyst for hydrogen generation. International Journal of Hydrogen Energy. 2014;39:2390-8.

[25] Ryu K, Zacharakis-Jutz GE, Kong S-C. Performance characteristics of compression-ignition engine using high concentration of ammonia mixed with dimethyl ether. Applied Energy. 2014;113:488-99.

[26] Reiter AJ, Kong S-C. Combustion and emissions characteristics of compression-ignition engine using dual ammonia-diesel fuel. Fuel. 2011;90:87-97.

[27] Reiter AJ, Kong S-C. Demonstration of compression-ignition engine combustion using ammonia in reducing greenhouse gas emissions. Energy & Fuels.

2008;22:2963-71.

[28] Mørch CS, Bjerre A, Gøttrup MP, Sorenson SC, Schramm J. Ammonia/hydrogen mixtures in an SI-engine: Engine performance and analysis of a proposed fuel system. Fuel. 2011;90:854-64.

[29] Haputhanthri SO, Maxwell TT, Fleming J, Austin C. Ammonia and Gasoline Fuel Blends for Spark Ignited Internal Combustion Engines. Journal of Energy Resources Technology. 2015;137:062201.

[30] Gross CW, Kong S-C. Performance characteristics of a compression-ignition engine using direct-injection ammonia–DME mixtures. Fuel. 2013;103:1069-79.

[31] Gray JT, Dimitroff E, Meckel NT, Quillian R. Ammonia Fuel-Engine Compatibility and Combustion. SAE Technical Paper; 1966.

[32] Grannell SM, Assanis DN, Bohac SV, Gillespie DE. The fuel mix limits and efficiency of a stoichiometric, ammonia, and gasoline dual fueled spark ignition engine. Journal of engineering for gas turbines and power. 2008;130:042802.

[33] Gill S, Chatha G, Tsolakis A, Golunski S, York A. Assessing the effects of partially decarbonising a diesel engine by co-fuelling with dissociated ammonia. International journal of hydrogen energy. 2012;37:6074-83.

[34] Frigo S, Gentili R. Analysis of the behaviour of a 4-stroke Si engine fuelled with ammonia and hydrogen. International journal of hydrogen energy. 2013;38:1607-15.

[35] El-Emam S, Desoky A. A study on the combustion of alternative fuels in spark-ignition engines. International journal of hydrogen energy. 1985;10:497-504.

[36] Comotti M, Frigo S. Hydrogen generation system for ammonia–hydrogen fuelled internal combustion engines. International Journal of Hydrogen Energy. 2015;40:10673-86.

[37] Mathieu O, Petersen EL. Experimental and modeling study on the high-temperature oxidation of Ammonia and related NOx chemistry. Combustion and Flame. 2015;162:554-70.

[38] Hiroyasu H, Kadota T, Arai M. Development and use of a spray combustion modeling to predict diesel engine efficiency and pollutant emissions: Part 1 combustion modeling. Bulletin of JSME. 1983;26:569-75.

[39] Dagaut P, Glarborg P, Alzueta MU. The oxidation of hydrogen cyanide and related chemistry. Progress in Energy and Combustion Science. 2008;34:1-46.

[40] Klippenstein SJ, Harding LB, Glarborg P, Miller JA. The role of NNH in NO formation and control. Combustion and Flame. 2011;158:774-89.

[41] Miller JA, Bowman CT. Mechanism and modeling of nitrogen chemistry in combustion. Progress in energy and combustion science. 1989;15:287-338.

[42] Kasuya F, Glarborg P, Johnsson JE, Dam-Johansen K. The thermal DeNOx process: Influence of partial pressures and temperature. Chemical Engineering Science. 1995;50:1455-66.

[43] Hohenberg GF. Advanced approaches for heat transfer calculations. SAE Technical Paper; 1979.

[44] Thoma M, Stiesch G, Merker G. Phänomenologisches Gemischbildungs-und Verbrennungsmodell zur Berechnung von Dieselmotoren mit Voreinspritzung. 5. Int Symp für Verbrennungsdiagnostik2002. p. 91-101.

국문초록

최근 몇 년 동안, 신재생 에너지 기술의 발달 및 확산과 함께 간헐적인 발전 특성을 보완하기 위한 에너지 저장 매체 기술개발이 필요하게 되었다. 이와 관련하여 수소는 에너지 저장 매체로 각광받고 있다. 그러나 수소는 매우 낮은 비등점을 갖기 때문에 액상으로 저장하는 것이 어렵고, 고압의 기체로 저장할 경우 단위 부피당 수소의 에너지 밀도가 현저히 낮다는 단점이 있다. 암모니아는 이러한 수소의 단점을 보완할 수 있는 에너지 저장 매체로서 최근 주목 받고 있다. 암모니아는 수소와 마찬가지로 탄소를 포함하지 않으므로 연소 시 탄소 관련 배출물을 생성하지 않으며 실온 및 10 기압의 조건에서 액상으로 존재하여 저장 및 운송에 장점이 있다.

이 박사논문에서는 이러한 신재생 에너지에 기반한 암모니아를 사용할 수 있는 가능성에 초점을 맞추어, 전기 및 기계적 에너지로의 재변환을 위해 고효율 저배기 내연기관의 새로운 연소전략을 제시하고 있다. 제시한 전략에서는 암모니아의 희박 예혼합 압축착화를 이용하여 얻은 고온 고압 조건을 활용하여 암모니아 주분사 연료의 연소를 가능하게 한다. 본 연구에서는 이러한 암모니아의 연소 전략을 이용하는 엔진의 운전 가능성과 연소 및 배출물 특성을 확인하기 위해 다영역 분무 모델을 활용한 엔진 모델 및 상세 화학반응 메커니즘을 개발하였다. 이러한 모델을 기반으로 다양한 주 분사시기 및 분사량 조건에서 모델링 분석을 수행하였다. 또한 암모니아 엔진의 주된 배출물인 질소산화물(NO) 생성 메커니즘을 분석하기 위해 주요 생성 및 파괴 반응 경로를 4 단계로 분류하고 다양한 분사시기 및 연료량 조건에서 NO 배출 특성을 분석하였다.

주요어 : 암모니아, 에너지저장매체, 내연기관, 연소전략, 엔진모델링

학 번 : 2011-20731